However, the strain-specific conformation of PrP^{Sc} and, in particular, its causal relationship with strain phenotypes, still remains controversial (13, 21).

Most of the information regarding strains so far available has been obtained from in vivo experiments using mice or hamsters, a system less advantageous for biochemical approaches to the molecular mechanisms of the strains. Neuronal cell culture models are clearly of greater value for such studies. However, only a few cultured cell lines, including PC12 and mouse neuroblastoma-derived N2a, have been shown to be permissive to scrapie agents (7, 26), and the levels of replication in these cell lines are not satisfactory, at least for quantitative detection of infectivity. Some of us previously demonstrated that cultured mouse neuronal cells expressing a high amount of PrP^{C} were highly permissive to replication of various mouse-adapted strains (15, 18). Arjona et al. recently compared two CJD strains using GT1-7 and N2a58 cells (1). The aim of the present study was to confirm the usefulness of the neuronal cell culture models by comparing phenotypes of mice inoculated with two strains, Chandler and Fukuoka-1. We report here that passage through the cell cultures did not change the strain-specific nature of the biological characteristics and discuss the relationship between strain phenotype and biochemical aspects of the PrP.

MATERIALS AND METHODS

Cell cultures. The mouse neuronal cell line GT1-7 (14) was exposed to mouse brain homogenates infected with each prion strain as described previously (15, 16, 18). The cells were cultured in DMEM containing heat-inactivated fetal bovine serum at 10% and penicillin-streptomycin and split every 5 days at a 1:3 ratio. All cultured cells were maintained at 37°C in 5% CO_2 in the biohazard prevention area of the authors' institution.

Mice. ddY mice used in the experiments were fed under specific-pathogen-free conditions. Experiments involving agent inoculation were conducted in the biohazard prevention area (P3) of the Laboratory Animal Center for Biomedical Research of the authors' institution.

Prion strains. The Fukuoka-1 strain (34) was passaged three times in the brains of ddY mice. The brains infected with Chandler strains were kindly donated by B. Caughey and R. Carp, respectively. The pooled brains were homogenized to 1% (wt/vol) in cold phosphate-buffered saline (PBS) containing 5% glucose. Cultured cell lysates were prepared by sonication in PBS. All of the homogenates and cell lysates were kept at −80°C until use.

Determination of LD_{50}. Confluent cell cultures in a 100-mm dish (approximately 7.5×10^6 cells) were sonicated in 0.5 ml of PBS. Before use, the cells were cultured for more than 30 passages following the initial ex vivo challenges. The cultured cell lysates and 1% (wt/vol) homogenates of brain tissues were serially diluted 10-fold with PBS, from 10^0 to 10^{-6}, and 20 μl of each dilution was inoculated into the right brain (five mice for each group). The inoculated mice were observed until 364 days after inoculation. The onset of disease was determined as previously described (28). The 50% lethal dose (LD_{50}) was determined according to the Behrens-Karber formula (10).

Histology. The brains were fixed in 4% paraformaldehyde and sectioned into 7-μm-thick sections at levels 250 and 500, as described by Sidman et al. (30). The tissue sections were stained with hematoxylin and eosin. The pattern of vacuolation was examined in 9 areas, namely the midbrain, hypothalamus, thalamus, hippocampus, paraterminal body, posterior cortex, cerebellar medulla, cerebellar granular layer, and cerebellar molecular layer. The vacuolation score was established based on the pattern, size, and density of the vacuoles using standard criteria from grade 0 for none and grade 5 for maximum vacuolation (9)

Antibodies. The anti-PrP polyclonal mouse antiserum used was described previously (19). The IBL-N rabbit antibody against N-terminal peptides of PrP and M20 goat antibody to C-terminal PrP peptides were purchased from Immuno Biological Laboratories (Gunma, Japan) and Santa-Cruz Biotech (Santa Cruz, CA), respectively. Horseradish peroxidase (HRP)-conjugated anti-mouse and -rabbit immunoglobulin G antibodies were purchased from Amersham. HRP-conjugated anti-goat immunoglobulin G antibodies were purchased from Santa-Cruz Biotech.

Immunoblotting. Confluent cultures were lysed for 30 min at 4°C in Triton-DOC lysis buffer (50 mM Tris-HCl [pH 7.5] containing 150 mM NaCl, 0.5% Triton X-100, 0.5% sodium deoxycholate, and 2 mM EDTA). After 1 min of centrifugation at 500 × *g*, the supernatant was collected and its total protein concentration was measured using the Bio-Rad protein assay. To detect PrP^{Sc}, the brain homogenates and cell lysates, with the protein concentration adjusted to 10 mg/ml, were treated with 100 μg/ml of proteinase K (Sigma) at 37°C for 30 min. To remove N-linked glycosylation, PNGase F was used according to the manufacturer's protocol (New England Biolabs) before PK digestion. The samples were boiled for 5 min in sodium dodecyl sulfate (SDS) loading buffer (50 mM Tris-HCl, pH 6.8, containing 5% glycerol, 1.6% SDS, and 100 mM dithiothreitol) and subjected to SDS–12% polyacrylamide gel electrophoresis. The proteins were transferred onto an Immobilon-P membrane (Millipore) in transfer buffer containing 15% methanol at 400 mA for 60 min, and the membrane was blocked with 5% nonfat dry milk in TBST (10 mM Tris-HCl [pH 7.8], 100 mM NaCl, 0.1% Tween 20) for 1 h at room temperature and reacted with anti-PrP antibodies. Immunoreactive bands were visualized by HRP-conjugated secondary antibodies using an enhanced chemiluminescence system (ECL; Amersham Pharmacia Biotech).

RESULTS

Biological characteristics of prion strains in cultured cells: clinical signs in inoculated mice. To examine the biological characteristics of the Chandler and Fukuoka-1 prion strains, GT1-7 cells independently infected with the two strains as well as infected mouse brain homogenates were inoculated into the brains of ddY mice. As shown in Table 1, all of the homogenates produced neurological symptoms and subsequent death in the inoculated mice. They exhibited some common clinical signs, such as weight loss, ruffled and greasy yellowish hair, tremor, hypersensitivity to sound and touch, and locomotor disturbance. However, all of the Chandler-infected mice were hyperactive at the early stages of the disease, in contrast to the progressive hypoactivity of Fukuoka-1-infected mice. When the mice at the terminal stages were sacrificed, a markedly extended bladder, due to urination disturbance, was observed in Fukuoka-1-inoculated, but not Chandler-inoculated, mice. These strain-specific symptoms were reproduced without exception in all of the mice, irrespective of whether brain homogenates or cultured cell lysates were used.

Incubation periods in inoculated mice. As shown in Table 1, the incubation periods of the mice inoculated with 1% brain homogenates of Fukuoka-1 and Chandler were 128.6 ± 9.9 days (mean ± standard deviation) and 149.8 ± 4.4 days, respectively. Interestingly, GT1-7 cells infected with Fukuoka-1 also exhibited a shorter incubation period than Chandler-infected cells: 139.7 ± 12.5 versus 150.2 ± 5.9 days. To analyze more quantitatively, the brain homogenates and GT1-7 cell lysates infected with Fukuoka-1 and Chandler, designated Fukuoka-1/brain, Chandler/brain, Fukuoka-1/GT1-7, and Chandler/GT1-7, respectively, were subjected to the end-point 10-fold dilution assay (Table 1). According to Behrens and Korber's formula, the infectious titers were estimated to be $10^{8.1}$ and $10^{8.8}$ LD_{50} units/g of the brain tissues and $10^{5.3}$ and $10^{6.5}$ LD_{50} units/10^7 GT1-7 cells infected with Fukuoka-1 and Chandler, respectively. After each dilution was converted to its infectious titer, the relationships between infectious titers and incubation periods in the four materials were analyzed. As shown in Fig. 1, plots of Fukuoka-1/brain and Fukuoka-1/GT1-7 clustered in the same region, and those of Chandler/brain and Chandler/GT1-7 formed another cluster located at the region representing much longer incubation periods. The linear relationships between infectious titers and incubation periods in brain homogenates and cell lysates in-

TABLE 1. Mortality and incubation periods of mice inoculated with prion strains[a]

Tissue or cell type	Fukuoka-1 strain			Chandler strain		
	Dilution	Mortality (no. dead/total)	Incubation period (days ± SD)	Dilution	Mortality (no. dead/total)	Incubation period (days ± SD)
Brain homogenate[b]	10^{-2}	5/5	128.6 ± 9.9	10^{-2}	5/5	149.8 ± 4.7
	10^{-3}	5/5	139.2 ± 8.9	10^{-3}	5/5	155.4 ± 7.1
	10^{-4}	5/5	145.6 ± 11.4	10^{-4}	5/5	183.4 ± 8.0
	10^{-5}	4/5	184.7 ± 25.7	10^{-5}	5/5	193.4 ± 16.8
	10^{-6}	4/5	250.5 ± 57.4	10^{-6}	3/5	204.0 ± 27.7
	10^{-7}	1/5	230.0	10^{-7}	4/5	248.0 ± 37.4
	10^{-8}	0/5		10^{-8}	0/5	
	10^{-9}	ND[d]		10^{-9}	0/5	
GT1-7 cell lysate[c]	10^{-0}	4/4	139.7 ± 12.5	10^{-0}	4/4	150.2 ± 5.9
	10^{-1}	5/5	137.2 ± 12.6	10^{-1}	4/4	167.3 ± 11.8
	10^{-2}	5/5	152.4 ± 10.0	10^{-2}	5/5	174.0 ± 10.5
	10^{-3}	5/5	199.4 ± 58.7	10^{-3}	5/5	193.6 ± 13.7
	10^{-4}	2/5	211.0 ± 4.2	10^{-4}	4/5	205.7 ± 18.5
	10^{-5}	0/5		10^{-5}	2/5	203.5 ± 27.5
	10^{-6}	0/5		10^{-6}	2/5	275.5 ± 71.4
	10^{-7}	0/5		10^{-7}	0/5	

[a] Twenty-microliter aliquots of serial 10-fold dilutions of GT1-7 cell lysates and brain homogenates (10^2, 1% [wt/vol] homogenate) were inoculated into the brain of a mouse. Inoculated cells were passaged 35 times before use.
[b] Infectious titers of the brain tissues infected with Fukuoka-1 and Chandler were $10^{8.1}$ and $10^{8.8}$ LD_{50} units/g tissue, respectively.
[c] Infectious titers of Fukuoka-1 and Chandler-infected GT1-7 cells were $10^{6.3}$ and $10^{6.5}$ LD_{50} units/10^7 cells, respectively.
[d] ND, not defined.

fected with each strain overlapped but were distinct between the strains (Fig. 1).

Pathological findings in inoculated mice. Brain sections including the hippocampus, thalamus, and cerebellum from inoculated mice at the terminal stage were stained with hematoxylin and eosin. As shown in Fig. 2, although spongiform change, neuronal loss, and gliosis are common characteristics of prion diseases, the severity and distribution of histological abnormalities differed between the brain tissues of Fukuoka-1- and Chandler-infected mice. In the Fukuoka-1-infected brains, large empty vacuoles were prominent mainly in the white matter, and a microcystic structure measuring up to 100 μm in diameter was observed in the cerebellar medulla (Fig. 2a and e). The grey matter was also affected in advanced cases, while the cerebellar granular and molecular layers were not damaged. The vacuoles in Chandler strain-infected brains were distributed equally in the grey and white matter. However, the number of vacuoles was fewer, and the size, an average of 27 μm in diameter, was obviously smaller than that of those from Fukuoka-1 strain-infected brains (Fig. 2b and f). In general, histopathological changes were much more severe in Fukuoka-1-infected tissues compared with those infected with the Chandler strain. These strain-specific pathological profiles were reproduced by inoculation of GT1-7 cell lysates infected with either strain (Fig. 2c, d, g, and h). A semiquantitative evaluation of the number and size of vacuoles (vacuolation score) in selected areas of brain tissues confirmed that the lesion profiles were strain specific (Fig. 3).

Biochemical aspects of PrP. Biochemical characteristics of PrP in the noninfected brain tissues and GT1-7 cells were

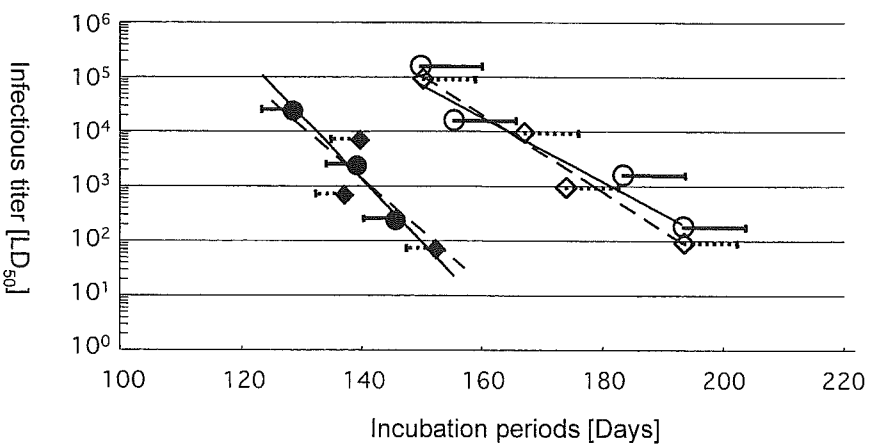

FIG. 1. Linear relationship between infectious titers and incubation periods. Each dilution used in the end-point assay shown in Table 1 was converted to its infectious titer, and the relationships between infectious titers (LD_{50}) and incubation periods (days) in Fukuoka-1/brain (closed circles), Chandler/brain (open circles), Fukuoka-1/GT1-7 (closed squares), and Chandler/GT1-7 (open squares) were analyzed. Horizontal bars indicate standard deviations.

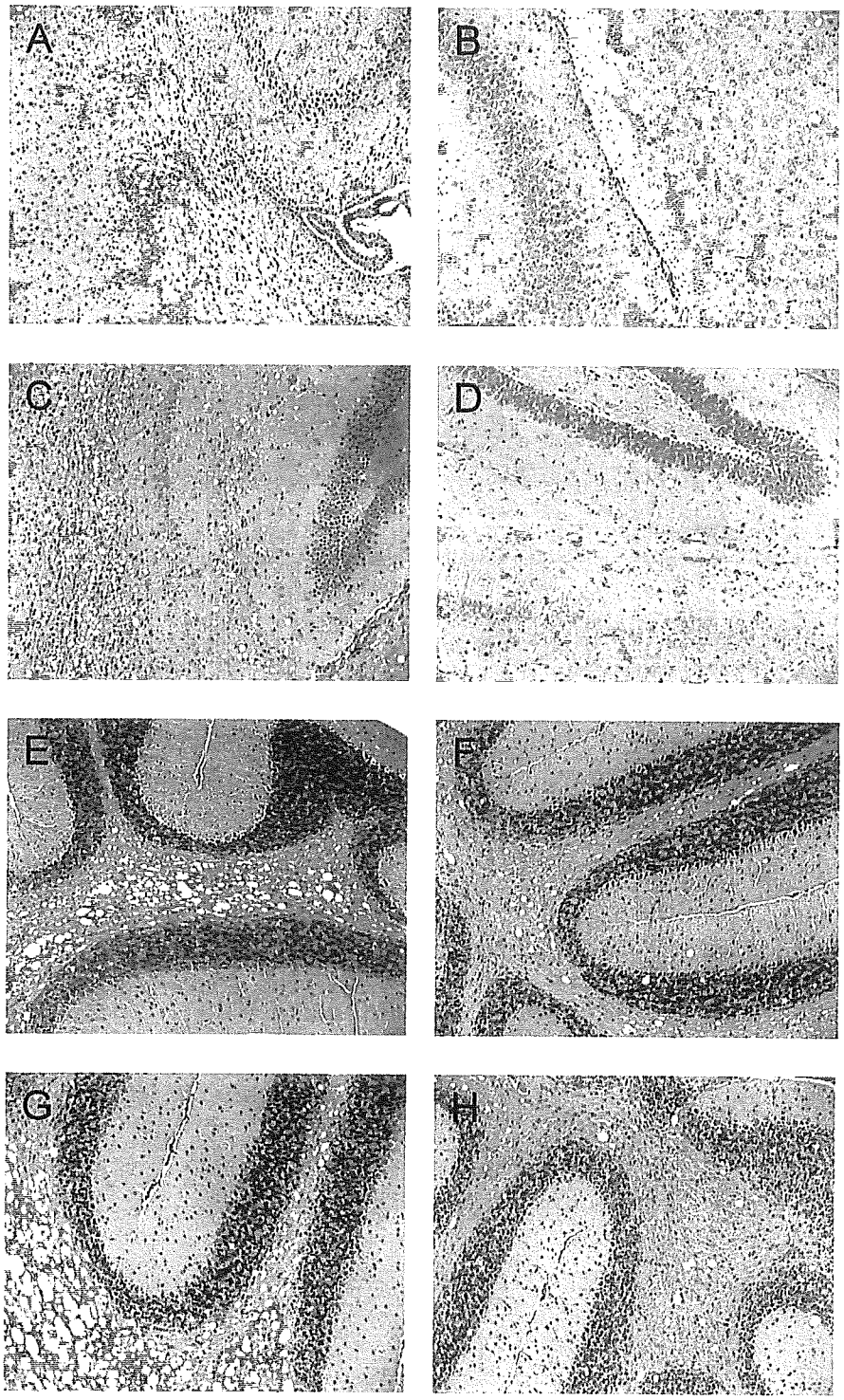

FIG. 2. Histological features of brain tissues infected with prion strains. Sections of the cerebrum (A to D) and cerebellum (E to H) of mice inoculated with Fukuoka-1/brain (A and E), Chandler/brain (B and F), Fukuoka-1/GT1-7 (C and G), and Chandler/GT1-7 (D and H) were stained with hematoxylin and eosin.

compared by immunoblotting. As shown in Fig. 4a, without PK treatment, the IBL-N antibody raised against N-terminal peptides of PrP visualized PrPs both in the noninfected brain and in GT1-7 cells. However, glycosylated components, a diglycosylated band in particular, of the latter migrated much more slowly, indicating that PrP in GT1-7 cells was more heavily glycosylated. Moreover, migration patterns of unglycosylated PrPs from the two sources also looked different: that in GT1-7 cells migrated a little faster. In the tissues and cells infected with Chandler and Fukuoka-1 strains, these host-specific char-

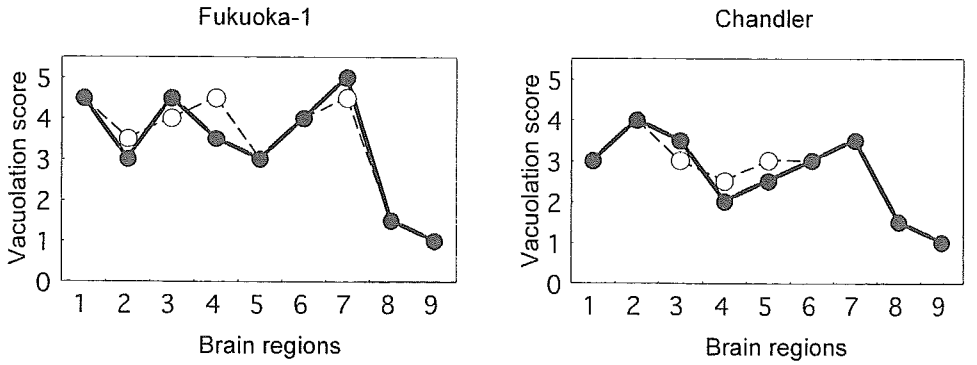

FIG. 3. Region profiles of vacuolation scores in infected mouse brain tissues. Scores were established based on the pattern, size, and density of vacuoles in the tissue using standard criteria with zero for none and five for maximum vacuolation. The pattern of vacuolation was examined in 9 areas, namely the midbrain (1), hypothalamus (2), thalamus (3), hippocampus (4), paraterminal body (5), posterior cortex (6), cerebellar medulla (7), cerebellar granular layer (8), and cerebellar molecular layer (9). Closed and open symbols indicate brain sections infected with brain homogenates and GT1-7 cell lysates, respectively. Each plot indicates the average score of sections from two mice.

acteristics of the PrP structure were essentially preserved. To confirm the difference in the migration patterns between unglycosylated PrPs from brain tissues and GT1-7 cells, Asn-linked glycosylation was completely removed by PNGase F treatment before immunoblotting. As shown in Fig. 4b, regardless of the presence or absence of prion infection, unglycosylated PrP from GT1-7 cells always migrated faster than that from brain tissues.

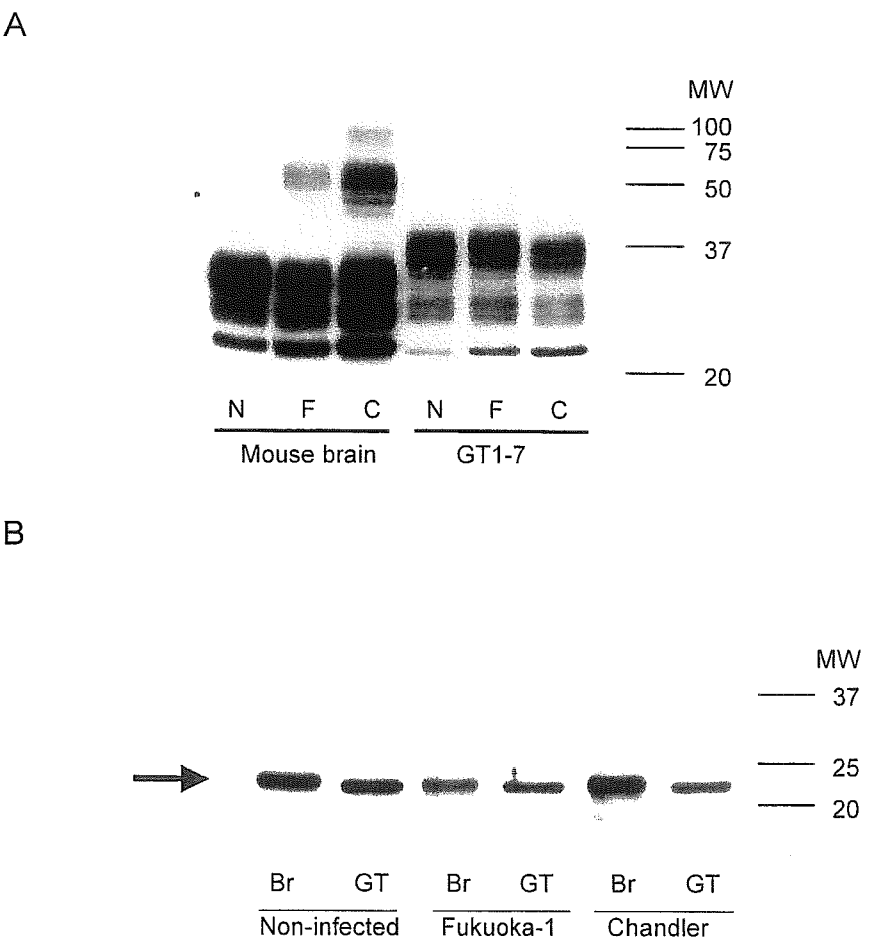

FIG. 4. Detection of PrP in brain homogenates and GT1-7 lysates without PK treatment. (A) Noninfected (N) brain homogenates and GT1-7 cell lysates and those infected with Fukuoka-1 (F) or Chandler (C) prions were subjected to immunoblotting with the IBL-N antibody against N-terminal PrP peptides. (B) The mobilities of nonglycosylated PrPs (arrow) from the brain tissues (Br) and GT1-7 cells (GT) were compared on an immunoblot with the IBL-N antibody after deglycosylation by PNGase F treatment. MW, molecular weight.

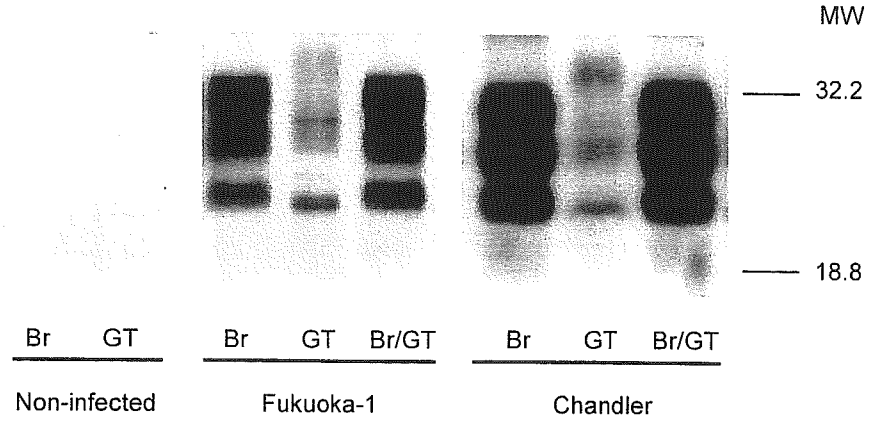

FIG. 5. Immunodetection of PK-resistant PrP in brain homogenates and GT1-7 lysates infected with prion strains. After treatment with PK, noninfected brain homogenates (Br) and GT1-7 cell lysates (GT) and those infected with Fukuoka-1 or Chandler prions were subjected to immunoblotting with polyclonal mouse antisera against PrP. The brain homogenates from terminal-stage mice inoculated with the lysates of GT1-7 cells infected with Fukuoka-1 or Chandler prions (Br/GT) were also analyzed. MW, molecular weight.

Strain-dependent differences in the biochemical aspects of PrP^{Sc}. PK completely digested PrP in the noninfected tissues and cells, while the resistant components (PrP^{Sc}) in the infected tissues and cells were visualized by polyclonal antiserum raised against a recombinant PrP (Fig. 5). Again, diglycosylated PrP^{Sc} in GT1-7 cells migrated to a much higher molecular mass, and its unglycosylated component migrated faster than PrP^{Sc} in the brain tissues. Of importance, PrP^{Sc} developed in the brain tissues of mice inoculated with the infected GT1-7 cell lysates had migration patterns that were indistinguishable from those of PrP^{Sc} in the original brain tissues. PNGase F treatment confirmed the different migration pat-

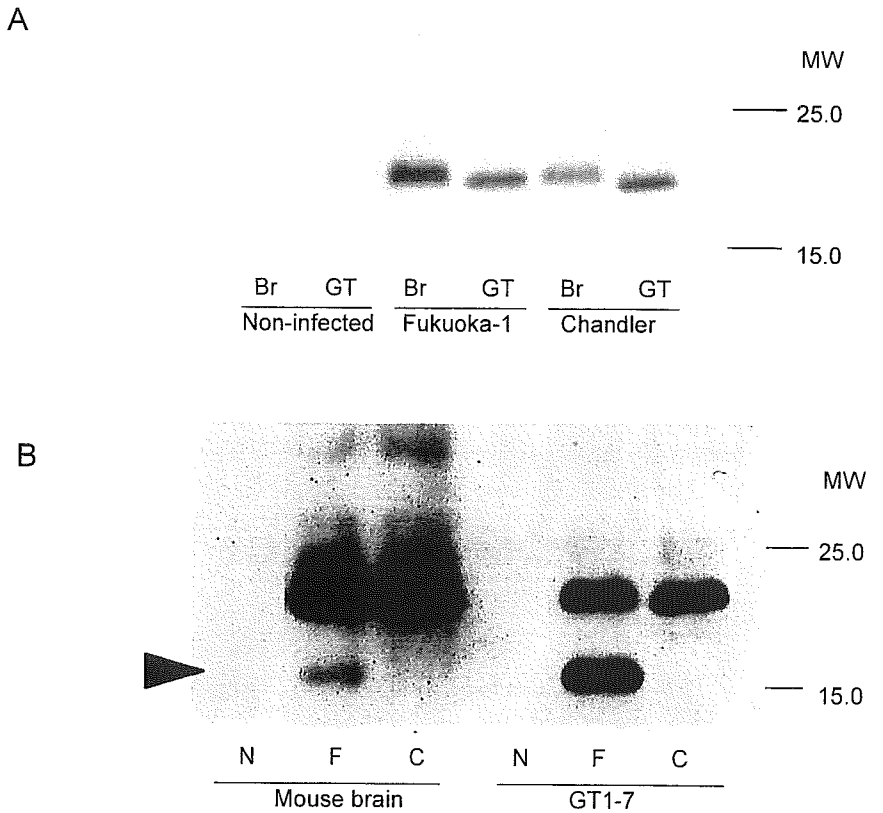

FIG. 6. Differences in the mobility of PK-resistant PrP between hosts and between strains. (A) After successive treatments with PK and PNGase F, mobilities in a gel of nonglycosylated PrP^{Sc} from the brain tissues (Br) and GT1-7 cells (GT) were compared on an immunoblot with the M20 antibody against C-terminal PrP peptides. (B) Mobilities of nonglycosylated PrP^{Sc} generated by Fukuoka-1 (F) and Chandler (C) strains are directly compared by immunoblotting with the M20 antibody. PrP in noninfected tissues and cells (N) is completely digested by PK. The arrowhead indicates the 13-kDa PrP fragment specifically found in the Fukuoka-1-infected tissues and cells. MW, molecular weight.

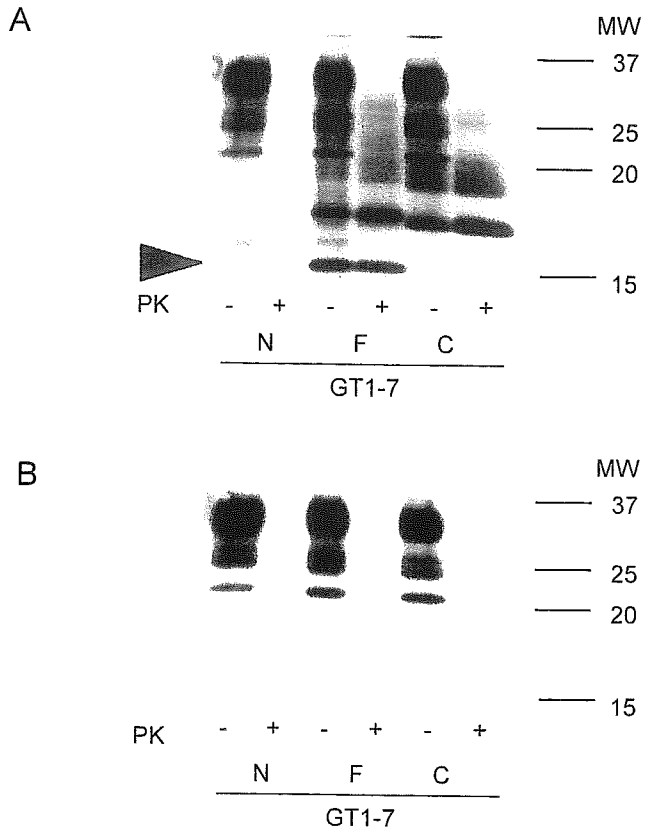

FIG. 7. The 13-kDa PrP fragment is detectable in Fukuoka-1-infected GT1-7 cells even without PK treatment. The cell lysates from noninfected (N) GT1-7 cells and those infected with the Fukuoka-1 (F) or Chandler (C) strain, with (+) or without (−) PK treatment, were subjected to immunoblotting using M20 (A) or IBL-N (B) anti-PrP antibodies. MW, molecular weight.

terns of unglycosylated PrP^{Sc} between the hosts (Fig. 6a). On the other hand, when migration patterns of PrP^{Sc} were directly compared between the strains in the same host on an immunoblot, Fukuoka-1-derived unglycosylated PrP^{Sc} clearly migrated more slowly than the Chandler-derived version (Fig. 6b). These findings strongly suggested that both host-specific and strain-specific factors are involved in the determination of the mobility of PK-resistant unglycosylated PrP^{Sc} in gel. Interestingly, in this immunoblotting, the M20 anti-C-terminal PrP antibody clearly visualized at a low molecular size, ~13 kDa, a component of PrP^{Sc} in Fukuoka-1-infected, but not Chandler-infected, GT1-7 cells (Fig. 5b). A faint but significant band of the 13-kDa fragments was also detectable in the Fukuoka-1-infected brain tissue. Since this fragment was similarly detectable even before the PK treatment and recognized by C-terminal (M20) but not N-terminal (IBL-N) PrP antibodies (Fig. 7), it is likely to be a C-terminal PrP fragment lacking a PK cleavage site.

DISCUSSION

Passage through the neuronal cell cultures of two prion strains, Chandler and Fukuoka-1, did not affect the biological characteristics, including clinical signs, incubation periods, and pathological findings, in the inoculated mice. Carryovers of the original strains into the cultures were unlikely, since the infected cells were cultured for more than 30 passages since the initial ex vivo challenges, assuming that residuals of original brain homogenates in the cultures would be diluted far greater than 10 orders of magnitude. We used a mouse neuronal cell line, GT1-7, which expresses a large amount of PrP^{C} and is highly permissive for replication of the agent (15, 18). Infected GT1-7 cells persistently produced PrP^{Sc} for more than 30 passages without subcloning and maintained high infectious titers of Fukuoka-1 and Chandler at the levels of $10^{5.3}$ and $10^{6.5}$ LD_{50} units/10^{7} cells, respectively. The high degree of competence in prion replication allowed us to quantify infectious titers in the cultured cells by end-point assay. Although data are not shown, we have found that the biological characteristics of the two strains, including clinical signs and incubation periods in the inoculated mice, are also conserved in other two neuronal cell lines, N2a58 (18) and 1C11 (17), which are permissive to various prion strains (16, 18; N. Nishida, unpublished). These findings are consistent with those of previous reports indicating that strain phenotypes did not change during several passages in cultured cells (1, 5).

Western blotting identified some differences in the biochemical features of PrP^{Sc} between the brain tissue and GT1-7 cells. The degrees of glycosylation of PrP^{Sc} derived from the two strains in GT1-7 cells were clearly higher than those in the brain tissues. A similar difference was observed before PK treatment even between the noninfected cells and tissues, suggesting the involvement of host cell factors rather than the strains. In some conditions, the degree of glycosylation (a ratio of glycoforms) of PrP^{Sc} is an important signature of the prion strain (5, 8). However, in our experimental models, it is largely determined by the hosts, presumably due to differences in the enzymatic activities involved in glycosylation or the trafficking pathway of de novo-synthesized PrP^{C}. Host cell- or tissue-determined PrP^{Sc} glycoforms have also been reported by others (31, 36). The mobility of unglycosylated PrP^{Sc} fragments in gel was also distinguishable between the brain tissues and GT1-7. This possibly reflected PK cleavage site heterogeneities due to the difference in the conformation of PrP^{Sc} or an artifact of experimental conditions such as pH (20). However, it is noteworthy that the size difference was also the case for PrP without PK treatment even between the noninfected tissues and cells, arguing against a difference in the PK cleavage sites. Sequencing of PrP cDNAs amplified by reverse transcription-PCR from the brain tissues and GT1-7 cells confirmed that their primary structures were identical (data not shown). A previous study identified, by use of mass spectrometry, six different glycosylphosphatidylinositol (GPI) glycoforms with molecular masses ranging from 2,670 to 3,285 Da in PrP^{Sc} purified from infected hamster brains as well as partially purified PrP^{C} (33). The presence of tissue-specific differences in the GPI composition was also suggested (12). Although the involvement of some difference in the PrP conformation preserved even in a denatured condition cannot be ruled out, a more likely explanation is that it is due to heterogeneity in the composition of GPI moieties. Precise mechanisms for the diversity in PrP structures among the hosts await elucidation, but these structural features are unlikely to affect the strain phenotype, which is shared by the hosts.

It has been hypothesized that the strain-specific conformation of PrP^{Sc} determines the pathological features and func-

tions as a template during pathogenic structural conversion of PrP^{C} to PrP^{Sc} in affected brain tissues (25). The present study also revealed evidence that some strain-specific features of the PrP^{Sc} band pattern on an immunoblot were conserved in the cultured cells. The unglycosylated PK-resistant PrP^{Sc} fragment derived from Fukuoka-1 always migrated more slowly than the Chandler-derived version accumulating in the same host, either in brain tissues or GT1-7 cells. So far, many prion strains, including those of human, sheep, and mink origin, have been characterized by the size of the PrP^{Sc} core fragment generated by PK (2–4, 24). In most cases, the size difference due to the diverse cleavage sites of PK is presumed to be a consequence of the extent of the β-sheet structure. However, Arjona et al. reported that identical PrP^{Sc} band patterns could be observed in GT1-7 cells infected with distinct CJD strains, FU and SY, but were different from those in brain tissues and N2a cells (1). This indicated that the conformational divergence of PrP^{SC} does not necessarily alter strain characteristics. We also demonstrated host-determined divergence, such as glycosylation patterns, which did not affect the biological characteristics of prion strains. Furthermore, the possible involvement of a putative agent or agent-induced factors other than the PrP^{Sc} conformation itself is not precluded. It would be of value to search for such factors that affect the mobility of PrP^{Sc} core fragment by using the cell culture model.

Strikingly, the small 13-kDa PrP^{Sc} fragment detected in Fukuoka-1-infected tissues and cells was not seen in Chandler-infected materials. It is likely that the 13-kDa. Fragment is strain-specific, since Fukuoka-1 but not Chandler resulted in the band not only in GT1-7 cells but also in N2a58 and 1C11 cells (N. Nishida, unpublished). It was PK resistant but detectable before PK treatment, suggesting a lack of PK cleavage sites and the involvement of endogenous proteolytic processes. It is possible that certain environmental factors, for instance, pH and metal ion concentration, influenced by the strain might alter the catalytic activities, but it is also possible that the Fukuoka-1-specific PrP^{Sc} conformation could allow endogenous proteases to access and catalyze the full-length PrP^{Sc}. Although both the Chandler and Fukuoka-1 strains are mouse-adapted ones, the former is of scrapie origin and the latter was derived from a GSS patient carrying the P102L mutation. One group previously demonstrated a similar 13-kDa fragment in the brain tissues from five of seven P102L GSS patients, and this fragment was immunoreactive to a C-terminal PrP antibody but not to 3F4 monoclonal antibody, indicating that it was N-terminally truncated beyond residue 112 (22). It would be intriguing to see whether the specific PrP^{Sc} conformation determined by a particular genetic mutation in the human brain tissues has been conserved during successive transmission to mouse brains and cultured cells lacking such a mutation. Some other reports demonstrated that PrP^{Sc} derived from F198S GSS and CJD also displayed patterns of endogenous proteolysis characteristic of each disorder, leading to distinct sets of PrP^{Sc} fragments (12). It is conceivable that different PrP^{Sc} fragments may exhibit unique biological and pathological consequences in the CNS. The most important pathological consequence of prion strains is the difference in the distribution of vacuolar degeneration among the CNS regions of affected animals. A possible explanation is that each prion strain possesses its own cell tropism. The investigation of cell tropism requires the stable infection of a single cell type which is permissive to more than one strain. In our preliminary experiments using the cell culture models, some strains revealed differential tropism among the cell types examined (N. Nishida, unpublished).

In conclusion, we demonstrated here that the prion strains tested conserved their biological characteristics following cell culture, and the accumulated PrP^{Sc} reproduced some specific features of its band pattern on an immunoblot. However, the molecular basis for conformational divergence of PrP^{Sc} is still enigmatic, and whether or not there is a causal relationship between the PrP^{Sc} conformation and strain phenotype remains to be concluded. Our cell culture models allow the analysis of trafficking and metabolism of PrP, i.e., posttranslational cleavage, glycosylation, recycling, and degradation, etc., which will provide a new insight into the understanding of the molecular basis of prion strains.

ACKNOWLEDGMENTS

We are grateful to Nobuhiko Okimura and Amanda Nishida for technical support and help in manuscript preparation, respectively.

R.A. is a research resident of a 21st Century Center of Excellence (COE) program of Japan. This work was supported by grants from the Ministry of Education, Culture, Sports, Science, and Technology, Japan, and the Ministry of Health, Labor, and Welfare, Japan.

REFERENCES

1. **Arjona, A., L. Simarro, F. Islinger, N. Nishida, and L. Manuelidis.** 2004. Two Creutzfeldt-Jakob disease agents reproduce prion protein-independent identities in cell cultures. Proc. Natl. Acad. Sci. USA **101:**8768–8773.
2. **Baron, T. G., and A. G. Biacabe.** 2001. Molecular analysis of the abnormal prion protein during coinfection of mice by bovine spongiform encephalopathy and a scrapie agent. J. Virol. **75:**107–114.
3. **Bartz, J. C., R. A. Bessen, D. McKenzie, R. F. Marsh, and J. M. Aiken.** 2000. Adaptation and selection of prion protein strain conformations following interspecies transmission of transmissible mink encephalopathy. J. Virol. **74:** 5542–5547.
4. **Bessen, R. A., and R. F. Marsh.** 1992. Biochemical and physical properties of the prion protein from two strains of the transmissible mink encephalopathy agent. J. Virol. **66:**2096–2101.
5. **Birkett, C. R., R. M. Hennion, D. A. Bembridge, M. C. Clarke, A. Chree, M. E. Bruce, and C. J. Bostock.** 2001. Scrapie strains maintain biological phenotypes on propagation in a cell line in culture. EMBO J. **20:**3351–3358.
6. **Bueler, H., A. Aguzzi, A. Sailer, R. A. Greiner, P. Autenried, M. Aguet, and C. Weissmann.** 1993. Mice devoid of PrP are resistant to scrapie. Cell **73:** 1339–1347.
7. **Butler, D. A., M. R. Scott, J. M. Bockman, D. R. Borchelt, A. Taraboulos, K. K. Hsiao, D. T. Kingsbury, and S. B. Prusiner.** 1988. Scrapie-infected murine neuroblastoma cells produce protease-resistant prion proteins. J. Virol. **62:**1558–1564.
8. **Collinge, J., K. C. Sidle, J. Meads, J. Ironside, and A. F. Hill.** 1996. Molecular analysis of prion strain variation and the aetiology of 'new variant' CJD. Nature **383:**685–690.
9. **Fraser, H., and A. G. Dickinson.** 1973. Scrapie in mice. Agent-strain differences in the distribution and intensity of grey matter vacuolation. J. Comp. Pathol. **83:**29–40.
10. **Gilles, H. J.** 1974. Calculation of the index of acute toxicity by the method of linear regression. Comparison with the method of "Karber and Behrens." Eur. J. Toxicol. Environ. Hyg. **7:**77–84.
11. **Hill, A. F., M. Desbruslais, S. Joiner, K. C. Sidle, I. Gowland, J. Collinge, L. J. Doey, and P. Lantos.** 1997. The same prion strain causes vCJD and BSE. Nature **389:**448–450, 526.
12. **Jimenez-Huete, A., P. M. Lievens, R. Vidal, P. Piccardo, B. Ghetti, F. Tagliavini, B. Frangione, and F. Prelli.** 1998. Endogenous proteolytic cleavage of normal and disease-associated isoforms of the human prion protein in neural and non-neural tissues. Am. J. Pathol. **153:**1561–1572.
13. **Manuelidis, L.** 2003. Transmissible encephalopathies: speculations and realities. Viral Immunol. **16:**123–139.
14. **Mellon, P. L., J. J. Windle, P. C. Goldsmith, C. A. Padula, J. L. Roberts, and R. I. Weiner.** 1990. Immortalization of hypothalamic GnRH neurons by genetically targeted tumorigenesis. Neuron **5:**1–10.
15. **Milhavet, O., H. E. McMahon, W. Rachidi, N. Nishida, S. Katamine, A. Mange, M. Arlotto, D. Casanova, J. Riondel, A. Favier, and S. Lehmann.** 2000. Prion infection impairs the cellular response to oxidative stress. Proc. Natl. Acad. Sci. USA **97:**13937–13942.

16. **Mouillet-Richard, S., M. Ermonval, C. Chebassier, J. L. Laplanche, S. Lehmann, J. M. Launay, and O. Kellermann.** 2000. Signal transduction through prion protein. Science **289**:1925–1928.
17. **Mouillet-Richard, S., V. Mutel, S. Loric, C. Tournois, J. M. Launay, and O. Kellermann.** 2000. Regulation by neurotransmitter receptors of serotonergic or catecholaminergic neuronal cell differentiation. J. Biol. Chem. **275**:9186–9192.
18. **Nishida, N., D. A. Harris, D. Vilette, H. Laude, Y. Frobert, J. Grassi, D. Casanova, O. Milhavet, and S. Lehmann.** 2000. Successful transmission of three mouse-adapted scrapie strains to murine neuroblastoma cell lines overexpressing wild-type mouse prion protein. J. Virol. **74**:320–325.
19. **Nishida, N., P. Tremblay, T. Sugimoto, K. Shigematsu, S. Shirabe, C. Petromilli, S. P. Erpel, R. Nakaoke, R. Atarashi, T. Houtani, M. Torchia, S. Sakaguchi, S. J. DeArmond, S. B. Prusiner, and S. Katamine.** 1999. A mouse prion protein transgene rescues mice deficient for the prion protein gene from purkinje cell degeneration and demyelination. Lab. Invest. **79**:689–697.
20. **Notari, S., S. Capellari, A. Giese, I. Westner, A. Baruzzi, B. Ghetti, P. Gambetti, H. A. Kretzschmar, and P. Parchi.** 2004. Effects of different experimental conditions on the PrPSc core generated by protease digestion: implications for strain typing and molecular classification of CJD. J. Biol. Chem. **279**:16797–16804.
21. **Parchi, P., S. Capellari, S. G. Chen, R. B. Petersen, P. Gambetti, N. Kopp, P. Brown, T. Kitamoto, J. Tateishi, A. Giese, and H. Kretzschmar.** 1997. Typing prion isoforms. Nature **386**:232–234.
22. **Parchi, P., S. G. Chen, P. Brown, W. Zou, S. Capellari, H. Budka, J. Hainfellner, P. F. Reyes, G. T. Golden, J. J. Hauw, D. C. Gajdusek, and P. Gambetti.** 1998. Different patterns of truncated prion protein fragments correlate with distinct phenotypes in P102L Gerstmann-Straussler-Scheinker disease. Proc. Natl. Acad. Sci. USA **95**:8322–8327.
23. **Parchi, P., and P. Gambetti.** 1995. Human prion diseases. Curr. Opin. Neurol. **8**:286–293.
24. **Parchi, P., W. Zou, W. Wang, P. Brown, S. Capellari, B. Ghetti, N. Kopp, W. J. Schulz-Schaeffer, H. A. Kretzschmar, M. W. Head, J. W. Ironside, P. Gambetti, and S. G. Chen.** 2000. Genetic influence on the structural variations of the abnormal prion protein. Proc. Natl. Acad. Sci. USA **97**:10168–10172.
25. **Prusiner, S. B.** 1998. Prions. Proc. Natl. Acad. Sci. USA **95**:13363–13383.
26. **Rubenstein, R., H. Deng, R. Race, W. Ju, C. Scalici, M. Papini, A. Rubenstein, R. Kascsak, and R. Carp.** 1994. Scrapie strain infection in vitro induces changes in neuronal cells. Mol. Neurobiol. **8**:129–138.
27. **Sakaguchi, S., S. Katamine, K. Shigematsu, A. Nakatani, R. Moriuchi, N. Nishida, K. Kurokawa, R. Nakaoke, H. Sato, K. Jishage, et al.** 1995. Accumulation of proteinase K-resistant prion protein (PrP) is restricted by the expression level of normal PrP in mice inoculated with a mouse-adapted strain of the Creutzfeldt-Jakob disease agent. J. Virol. **69**:7586–7592.
28. **Sakaguchi, S., S. Katamine, K. Yamanouchi, M. Kishikawa, R. Moriuchi, N. Yasukawa, T. Doi, and T. Miyamoto.** 1993. Kinetics of infectivity are dissociated from PrP accumulation in salivary glands of Creutzfeldt-Jakob disease agent-inoculated mice. J. Gen. Virol. **74**:2117–2123.
29. **Scott, M., D. Foster, C. Mirenda, D. Serban, F. Coufal, M. Walchli, M. Torchia, D. Groth, G. Carlson, S. J. DeArmond, et al.** 1989. Transgenic mice expressing hamster prion protein produce species-specific scrapie infectivity and amyloid plaques. Cell **59**:847–857.
30. **Sidman, R. L., J. B. Angevine, Jr., and E. T. Pierce.** 1971. Atlas of the mouse brain and spinal cord. Harvard University Press, Cambridge, Mass.
31. **Somerville, R. A.** 1999. Host and transmissible spongiform encephalopathy agent strain control glycosylation of PrP. J. Gen. Virol. **80**:1865–1872.
32. **Somerville, R. A., A. Chong, O. U. Mulqueen, C. R. Birkett, S. C. Wood, and J. Hope.** 1997. Biochemical typing of scrapie strains. Nature **386**:564.
33. **Stahl, N., M. A. Baldwin, R. Hecker, K. M. Pan, A. L. Burlingame, and S. B. Prusiner.** 1992. Glycosylinositol phospholipid anchors of the scrapie and cellular prion proteins contain sialic acid. Biochemistry **31**:5043–5053.
34. **Tateishi, J., M. Ohta, M. Koga, Y. Sato, and Y. Kuroiwa.** 1979. Transmission of chronic spongiform encephalopathy with kuru plaques from humans to small rodents. Ann. Neurol. **5**:581–584.
35. **Telling, G. C., P. Parchi, S. J. DeArmond, P. Cortelli, P. Montagna, R. Gabizon, J. Mastrianni, E. Lugaresi, P. Gambetti, and S. B. Prusiner.** 1996. Evidence for the conformation of the pathologic isoform of the prion protein enciphering and propagating prion diversity. Science **274**:2079–2082.
36. **Vorberg, I., and S. A. Priola.** 2002. Molecular basis of scrapie strain glycoform variation. J. Biol. Chem. **277**:36775–36781.

Science

Reciprocal Interference Between Specific CJD and Scrapie Agents in Neural Cell Cultures

Noriuki Nishida, Shigeru Katamine, Laura Manuelidis

21 October 2005, Volume 310, pp. 493-496

Reciprocal Interference Between Specific CJD and Scrapie Agents in Neural Cell Cultures

Noriuki Nishida,[1,2] Shigeru Katamine,[3] Laura Manuelidis[1]*

Infection of mice with an attenuated Creutzfeldt-Jakob disease agent (SY-CJD) interferes with superinfection by a more virulent human-derived CJD agent (FU-CJD) and does not require pathological prion protein (PrPres). Using a rapid coculture system, we found that a neural cell line free of immune system cells similarly supported substantial CJD agent interference without PrPres. In addition, SY-CJD prevented superinfection by sheep-derived Chandler (Ch) and 22L scrapie agents. However, only 22L and not Ch prevented FU-CJD infection, even though both scrapie strains provoked abundant PrPres. This relationship between particular strains of sheep- and human-derived agents is likely to affect their prevalence and epidemic spread.

In transmissible spongiform encephalopathies (TSEs) such as human CJD, sheep scrapie, and bovine spongiform encephalopathy (BSE), B and T cell adaptive immune responses to a foreign infectious agent have not been detected (*1*). Nonetheless, an attenuated CJD agent, designated SY, was able to prevent superinfection by the more virulent and rapidly lethal FU-CJD agent (*2*). These experiments exploited two human CJD agents that, when passaged in mice, were readily distinguished by profound differences in the incubation time to disease and the distribution of brain lesions. The attenuated "slow" SY produced only small medial thalamic lesions typical of sporadic CJD in mice, whereas the virulent "fast" FU strain, isolated only in Japan, caused widespread severe lesions with many amyloid deposits (Table 1). Clear protective effects of SY-CJD against superinfection by FU-CJD were demonstrable with both intracerebral and peripheral challenges, and SY-protected mice could live free of disease for >600 days, a typical mouse life span (*3*, *4*). By comparison, there was minimal interference between scrapie strains 22C and 22A (*5*). This raised the possibility that protective effects might be restricted to particular strains of CJD or to unusual agent strain combinations. We sought ways to evaluate interference between different combinations of TSE agents, and to determine whether apparently unrelated agents—such as those propagated from human CJD and from sheep scrapie cases—could be antagonistic.

Mice can respond to CJD agents through a variety of myeloid cell and innate defense mechanisms (*6*–*8*). Thus, it was relevant to determine whether different agent strains could prevent superinfection in simplified cell cultures that lack B, T, and myeloid cells. Neural cells, which can be susceptible to TSE agents, would be incapable of producing many of the myeloid cell cytokines that can participate in strain interference in vivo. If interference could be demonstrated in neural cells, it would show that more universal cellular pathways are sufficient for protection. These culture models also might be used to identify crucial, and possibly novel, molecular pathways of innate immunity to TSE agents.

We developed a rapid, simple, and flexible test of interference in GT1-7 cells (hereafter called GT cells), a murine hypothalamic cell line. We previously found that these cells support the replication of a variety of mouse-passaged CJD and scrapie agents (Table 1) (*9*, *10*). A neomycin-resistant plasmid was introduced into the target GT cells (GTneo) to allow their selection by G418 antibiotic treatment (*11*) (Fig. 1). Infected GT challenge cells were killed by adding G418 to cocultures, and the pure GTneo target cells were then passaged and assayed for PrPres, a surrogate marker for infection in GT cells. Although PrPres does not quantitatively correlate with infectious

[1]Yale Medical School, New Haven, CT 06510, USA. [2]Center for Emerging Infectious Diseases, Gifu University, Yanagido 1-1, Gifu 501-1193, Japan. [3]Department of Molecular Microbiology and Immunology, Nagasaki University Graduate School of Medicine, 1-12-4 Sakamoto, Nagasaki 852-8523, Japan.

*To whom correspondence should be addressed. E-mail: laura.manuelidis@yale.edu

Table 1. Cell lines and TSE agents for testing interference. Agents, their source, and the number of cell passages after infection at the time of challenge are shown. By convention, TSE agent names identify the natural host. Thus, scrapie agents are derived from sheep, CJD agents from humans, CWD agents from cervids, and BSE agents from cows. Hence, the terms mouse scrapie and PrP^{Sc} (i.e., PrPres in mice infected with scrapie) indicate infection with sheep-derived agents. The UK Chandler (Ch) "drowsy" strain [equivalent to Rocky Mountain Laboratory (RML) scrapie], from a goat with experimental scrapie, is distinct from 22L scrapie (typical scratching scrapie in sheep from brain pool SSBP1). These scrapie strains are clearly different from CJD and BSE agents propagated in mice (i.e., their separate identities are not made homogeneous by the murine host). CJD encompasses all subsets of human TSE infectious agents except kuru, including those isolated from patients with PrP mutations such as PrP 102L of Gerstmann-Sträussler-Sheinker disease (GSS). SY-CJD causes circumscribed thalamic lesions only after ≥350 days in mice, and it is representative of sporadic CJD agents in the Western hemisphere, including agents isolated from GSS patients (*23*). No CJD agent similar to the representative Japanese fast FU-CJD agent ("CJD-Fukuoka-1") that induces widespread PrP amyloid deposits and severe demyelination has ever been isolated outside of Japan. Because FU-CJD and the Ch and 22L scrapie strains all cause widespread brain pathology, interference between these strains cannot be assessed in mice.

Cell line	Agent strain	Origin	Passages
GT (GT1-7)	—	—	—
SY+GT	SY	CJD sporadic: USA	≥106
FU+GT	FU	CJD (GSS 102L): Japan	≥110
Ch+GT	Ch	"Drowsy" scrapie: UK	≥50
22L+GT	22L	"Scratching" scrapie: UK	≥50
GTneo	Mock	—	≥15
SY+GTneo	SY	CJD sporadic: USA	≥110
Ch+GTneo	Ch	"Drowsy" scrapie: UK	≥15
22L+GTneo	22L	"Scratching" scrapie: UK	≥15

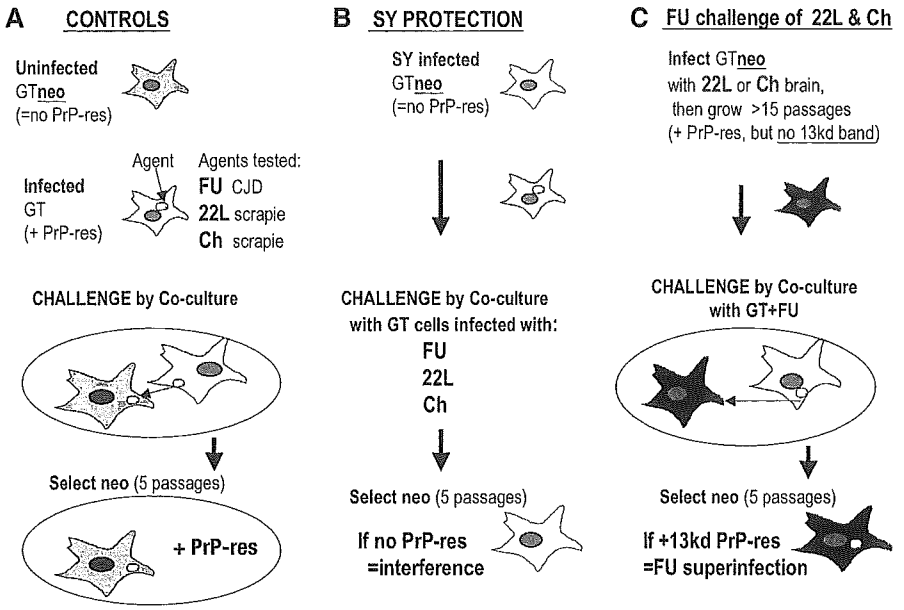

Fig. 1. In vitro interference strategy: Coculture challenges of (**A**) uninfected control cells, (**B**) SY-infected cells, and (**C**) scrapie-infected cells. Target GTneo cells were challenged with mock GT or infected GT cells by coculture for 2 days. GT challenge cells were then killed by G418 treatment, and resistant GTneo cells were analyzed for PrPres (*11*). For FU challenges, GTneo cells were newly infected with 22L or Ch scrapie brain homogenates and passaged >15 times before coculture.

titers, and may not be detectable in all infectious samples [e.g., (*1*, *4*, *12*, *13*)], its presence does indicate infection in GT cells (*10*).

GTneo target cells were exposed to uninfected brain tissue or to equal numbers of uninfected donor cells (i.e., mock-infected as in Fig. 1A). Such control GTneo cells should fail to produce PrPres. In contrast, mock-infected GTneo cells challenged with infected GT cells should become persistently infected and display PrPres long after the GT cells are removed by G418 treatment. Challenges of GTneo cells by GT cells infected with the agents 22L scrapie (GT+22L), Ch scrapie (GT+Ch), or FU-CJD (GT+FU) were rapidly effective (Fig. 2A). A large amount of PrPres was produced by all the control target cells after challenge with infected GT cells, but no PrPres was present after exposure to uninfected brain tissue (in this and in three or more repeat experiments per condition). Further in vitro passages of these GTneo target cells showed stable production of PrPres, indicating persistent infection by each of the challenge agents. Some TSE agents have been associated with variant PrPres band patterns (*14*). The three major PrPres bands were the same in all infected cells. However, an extra, highly reproducible, 13-kD band of PrPres was seen only in FU-infected cells. Antibodies identified this as a C-terminal PrPres fragment (Fig. 2A, C-13). Because this band was not present with any of the other agents, we could use it to specifically diagnose FU superinfection. Moreover, with all challenge agents, rapid infection with de novo production of large amounts of PrPres was apparent by 25 days in culture, whereas intracerebral inoculation with FU homogenates takes more than 90 days to induce brain PrPres (*8*).

In parallel with these controls, we tested whether SY could interfere with FU superinfection in culture as it does in mice, and we also tested whether SY infection could reduce susceptibility to presumably unrelated scrapie agents (Fig. 1B). The neomycin plasmid was added to PrPres-negative but persistently infected SY cells (as verified by repeated bioassays) (*10*, *11*). The lack of PrPres in SY-infected target cells greatly simplified the interference assay. After challenge, a continued lack of PrPres would indicate that covert SY infection protected cells from superinfection. In all these experiments, the number of infectious particles in challenge cells was higher than in target cells by a factor of ≥10,000 (*11*). No PrPres was detected in the GTneo+SY cells challenged with 22L cells (SY/22L lane, Fig. 2B). Thus, SY infection interfered with 22L superinfection. G418 selection also visibly removed all of the abundant PrPres of challenge cells. Persistent SY infection additionally interfered with GT+Ch scrapie agent and GT+FU CJD agent challenges. Only a barely detectable smear of signal was seen in the PrPres gel region (Fig. 2B). Moreover, the 13-kD PrPres band elicited by FU infection was never detectable in the FU-challenged SY cells, and the lack of any distinguishing strain-specific PrPres patterns for the other three common major PrPres bands made it impossible to determine whether the ± signal was due to low levels of the challenge strain. Two repeat experiments reconfirmed that SY interfered with superinfection by 22L, Ch, and FU agents (Table 2). Although the PrPres results do not permit us to conclude that there was complete prevention of superinfection, the interference of SY against 22L, Ch, and FU agents in vitro was manifest, and in marked contrast to the results with unprotected cells.

Because the 13-kD PrPres band was seen only after FU infection (Fig. 2A), it was possible to test whether scrapie agents could protect against the FU-CJD agent (Fig. 1C). We established new persistent infections of GTneo cells by standard application of infected brain homogenates (*9*, *10*), and verified that these newly infected GTneo cells continued to produce substantial amounts of

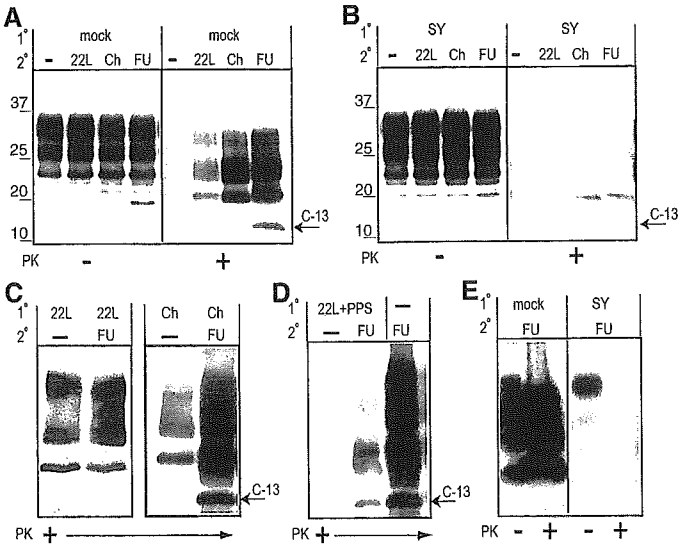

Fig. 2. Immunoblots of control and infected target cells. (**A**) Challenge of mock-infected and (**B**) SY-CJD–infected GTneo target cells by coculture with uninfected GT cells (–) or with infected GT+22L, GT+Ch, and GT+FU cells. Primary agent (1°) and challenge agent (2°) are indicated with total PrP compared to PrPres after limited proteinase K (PK) digestion. No PrPres is detectable in SY-infected cells, and the C-13 band is seen only in FU-infected cells. Markers (in kilodaltons) are at left. (**C**) PrPres after mock (–) and FU-CJD challenge (FU) of 22L scrapie GTneo cells (left) versus challenge of Ch scrapie GTneo cells (right). Mock controls (–) both show high levels of PrPres in scrapie-infected cells before FU challenge. After FU challenge of 22L cells, the pattern and amount of PrPres is unchanged, indicating no appreciable superinfection, and the C-13 band is undetectable. In contrast, massive superinfection by FU is apparent in Ch-infected cells, with markedly increased PrPres and a clear 13-kD band (C-13). (**D**) Superinfection of "cured" 22L cells treated with pentosan polysulfate (22L+PPS). PrPres is not detectable in the "cured" unchallenged cells (left lane) as compared with the original 22L-infected cells in (C). "Cured" cells challenged with FU became susceptible to FU superinfection and showed the C-13 FU diagnostic band (middle lane, arrow). The "cured" cells, however, showed less PrPres than did the parallel FU-challenged uninfected controls (right lane), possibly suggesting residual 22L scrapie agent. (**E**) Mock- and SY-infected target cells (minus neo plasmid or G418 selection) challenged with GT+FU cells separated by a 0.4μ filter. Mock cells became infected (positive for PrPres, left), whereas SY-infected cells were protected (right). C-13 is not seen in whole-cell lysates (*11*).

Table 2. Interference results in three replicate experiments. Symbols: +, strong PrPres signal (positive infection); –, no detectable PrPres; ±, barely detectable or questionable PrPres signal between 19 and 30 kD. C-13 is the FU diagnostic band. FU-CJD, 22L, and Ch scrapie infectious challenges were of greater magnitude than in previous in vivo studies (*11*).

Agent		PrPres		Interference
1° first	2° challenge	19 to 30 kD	C-13	
Mock	FU-CJD	+ / + / +	+ / + / +	No
Mock	22L scrapie	+ / + / +	– / – / –	No
Mock	Ch scrapie	+ / + / +	– / – / –	No
SY-CJD	Mock	– / – / –	– / – / –	—
SY-CJD	FU-CJD	± / – / –	– / – / –	Yes
SY-CJD	22L scrapie	– / ± / ±	– / – / –	Yes
SY-CJD	Ch scrapie	± / – / –	– / – / –	Yes
22L scrapie	FU-CJD	+ / + / +	– / – / –	Yes
Ch scrapie	FU-CJD	+ / + / +	+ / + / +	No

pathologic PrPres for >15 in vitro passages before challenging them with GT+FU cells. Both the 22L and Ch scrapie–infected GTneo cells, but not the parallel mock-infected cells, showed large amounts of the three major PrPres bands, but not the extra 13-kD band that was diagnostic for FU infection. These 22L and Ch scrapie–infected GTneo cells were then challenged with FU+GT cells that displayed the 13-kD band (as in Fig. 2A). A large increase in PrPres and/or the appearance of the extra 13-kD PrPres band in scrapie-infected GTneo cells would show that these particular scrapie agents failed to prevent superinfection by FU. Superinfection would also prove that high levels of PrPres are not protective.

The scrapie strains 22L and Ch displayed markedly different capacities for interfering with FU superinfection (Fig. 2C). Target 22L cells were protected against FU superinfection. The PrPres intensity and band patterns of 22L cells exposed to FU (22L/FU lane, Fig. 2C) were the same as in 22L controls (22L/– lane), and the lack of the FU-diagnostic 13-kD PrPres band further confirmed that only the initial 22L infection was present. The 13-kD PrPres band also did not appear with additional in vitro passages, indicating that FU was probably not covertly contaminating the target cells. These results were reproducible (Table 2).

In sharp contrast, Ch scrapie infection did not protect GTneo cells from FU superinfection. PrPres accumulation in these FU-challenged cells (Ch/FU lane, Fig. 2C) was considerably more intense than in mock cells (Ch/– lane), and consistent with the amount of pathologic PrPres that would be provoked by infection with both agents. Additionally, there was a strong 13-kD PrPres signal indicating FU superinfection (Fig. 2C and Table 2). Hence, enormous amounts of PrPres provoked by the Ch agent did not prevent massive superinfection by a second strain. Because in situ studies show that FU infects most GT cells (*10*), it is likely that a fair proportion of the Ch/FU cells were doubly infected. Brain tissue can also be doubly infected, and each agent breeds true despite cocultivation in that tissue for >200 days (*3*). In sum, two scrapie strains eliciting the same PrPres band pattern show markedly different susceptibilities to a CJD agent that provokes an extra PrPres band.

To further show that interference depended on persistent infection, we "cured" GT+22L neo cells by treating them with pentosan polysulfate (*11*) until PrPres was undetectable (Fig. 2D). We then challenged these "cured" 22L cultures and parallel mock controls with GT+FU as above. These "cured" cultures became susceptible to FU superinfection and showed the diagnostic FU 13-kD band (Fig. 2D), unlike the 22L-protected cells (Fig. 2C). This experiment also shows that the 22L agent, rather than some new cellular characteristic induced by neo plasmid/G418 selection, was the ultimate cause of interference.

Direct cell-to-cell contacts may aid agent transmission in vivo, as in the transfer of infectious agent from follicular dendritic cells to transiting white blood cells (*15*). We found that concentrated supernatants from both 22L- and FU-infected GT cells were less infectious than the remaining whole washed cells by a factor of ~1000, as measured by bioassay. We also prevented direct cell-to-cell contact with 0.4μ filters placed between challenge cells and GT+SY target (minus neoplasmid) cells. This would permit the transit of large viruses and aggregates but not whole cells. Equal numbers of healthy challenge and target cells were plated and exposed for 2 days, and the separated target cells were then passaged and analyzed (*11*). Target control cells required ≥8 in vitro passages to produce PrPres and did not always become positive, unlike the cocultures described above. However, despite this caveat, SY infection did interfere with FU superinfection as compared to more typical controls (Fig. 2E). Thus, SY infection rather than neo transformation and G418 selection was the primary cause of interference.

We have shown that infected neural cells in culture carry all the requisite features for

mounting a substantial TSE interference effect. No immune system cells were necessary for this protection, and stable interfering infections were reproducibly achieved without cloning. Interference did not depend on the presence or absence of abnormal PrP. Only persistent infection protected target cells from superinfection. Additionally, only particular agent-strain combinations showed positive interference, and these could not be predicted from cellular PrPres amounts or banding patterns. Moreover, despite continuous replication in cells with PrPres band patterns very different from those found in brain tissue, SY and FU CJD agents each breed true when reinoculated into mice, as does rodent-passaged scrapie reinoculated in sheep (*10*). The stability of the BSE agent also contrasts with the many different PrPres patterns seen in various affected species. Together, these results are not compatible with the common assumption that TSE strains are encoded by some unresolved type of PrPres folding (*16*, *17*). Indeed, there is still no conclusive evidence that any recombinant or amplified form of abnormal PrP can infect normal animals directly, reproduce meaningful levels of infectivity, or encode all the strain differences observed in mice infected with scrapie, CJD, and BSE agents.

Unlike heterogeneous aggregates of pathological PrP, infectious TSE particles have a discrete viral size of ~25 nm and 10^7 daltons (as assessed by field flow fractionation and high-pressure liquid chromatography, respectively) (*18*), and releasing their tightly bound nucleic acids destroys infectivity (*19*). Thus, some TSE agents such as SY may produce defective interfering particles, as found in many persistent viral as well as noncoding human viroid infections (*20*, *21*). Unlike pathologic host PrP, TSE agents can also provoke innate cellular defenses, including intracellular and diffusible factors that are not restricted to immune system cells (*7*, *8*), and such factors are likely to be involved in interference. Small interfering RNAs with extensive secondary structure may also be evoked by TSE agents, and these can provide even greater strain specificity (*22*). Notably, several small RNAs with extensive secondary structure have been identified in TSE-infected but not in normal brain tissue (*23*), and such motifs deserve further study in TSE culture models.

Cocultures were more efficient than mouse bioassays and can be useful for rapid assessment of agent purification and recovery (*24*). Additionally, they may provide a sensitive test for cells that are infected but show no PrPres (such as white blood cells), and they may be useful for evaluating a wide range of evolving TSE agents that have become important epidemiologically, such as those that cause BSE and chronic wasting disease (CWD). The resistance of cells infected with a prototypic sporadic CJD agent (SY) to two scrapie strains supports the suggestion that a commensal but rarely pathogenic TSE agent may help protect people against infection by sheep TSE strains in nature (*4*), and may explain why so few people have developed BSE-linked CJD (*25*). The clustering of sporadic CJD cases is also consistent with an environmental agent of low virulence (*26*).

References and Notes

1. L. Manuelidis, W. Fritch, Y. G. Xi, *Science* **277**, 94 (1997).
2. L. Manuelidis, *Proc. Natl. Acad. Sci. U.S.A.* **95**, 2520 (1998).
3. L. Manuelidis, Z. Y. Lu, *Neurosci. Lett.* **293**, 163 (2000).
4. L. Manuelidis, Z. Y. Lu, *Proc. Natl. Acad. Sci. U.S.A.* **100**, 5360 (2003).
5. A. Dickinson, H. Fraser, V. Meikle, G. Outram, *Nature New Biol.* **237**, 244 (1972).
6. C. Baker, L. Manuelidis, *Proc. Natl. Acad. Sci. U.S.A.* **100**, 675 (2003).
7. C. Baker, Z. Lu, L. Manuelidis, *J. Neurovirol.* **10**, 1 (2004).
8. Z. Lu, C. Baker, L. Manuelidis, *J. Cell. Biochem.* **93**, 644 (2004).
9. N. Nishida *et al.*, *J. Virol.* **74**, 320 (2000).
10. A. Arjona, L. Simarro, F. Islinger, N. Nishida, L. Manuelidis, *Proc. Natl. Acad. Sci. U.S.A.* **101**, 8768 (2004).
11. See supporting data on *Science* Online.
12. C. Lasmezas *et al.*, *Science* **275**, 402 (1997).
13. Y. G. Xi, A. Ingrosso, A. Ladogana, C. Masullo, M. Pocchiari, *Nature* **356**, 598 (1992).
14. A. Hill *et al.*, *Brain* **126**, 1333 (2003).
15. L. Manuelidis *et al.*, *J. Virol.* **74**, 8614 (2000).
16. S. Prusiner, *Proc. Natl. Acad. Sci. U.S.A.* **95**, 13363 (1998).
17. G. S. Jackson, J. Collinge, *Mol. Pathol.* **54**, 393 (2001).
18. T. Sklaviadis, R. Dreyer, L. Manuelidis, *Virus Res.* **3**, 241 (1992).
19. L. Manuelidis, T. Sklaviadis, A. Akowitz, W. Fritch, *Proc. Natl. Acad. Sci. U.S.A.* **92**, 5124 (1995).
20. A. Barrett, *Curr. Top. Microbiol. Immunol.* **128**, 55 (1986).
21. J. Wu *et al.*, *World J. Gastroenterol.* **11**, 1658 (2005).
22. P. M. Waterhouse, M. B. Wang, T. Lough, *Nature* **411**, 834 (2001).
23. L. Manuelidis, in *Transmissible Subacute Spongiform Encephalopathies: Prion Diseases*, L. Court, B. Dodet, Eds. (Elsevier, Paris, 1966), pp. 375–387.
24. L. Manuelidis *et al.*, unpublished data.
25. L. Linsell *et al.*, *Neurology* **63**, 2077 (2004).
26. P. Smith, S. Cousens, J. d'Huillard Aignaux, H. Ward, R. Will, *Curr. Top. Microbiol. Immunol.* **284**, 161 (2004).

27. Supported by NIH grant NS12674, U.S. Department of Defense grant DAMD-17-03-1-0360, and a grant from the Ministry of Health, Labor and Welfare, Japan.

Supporting Online Material

www.sciencemag.org/cgi/content/full/310/5747/493/DC1

Materials and Methods

29 July 2005; accepted 21 September 2005
10.1126/science.1118155

Neuroscience 136 (2005) 281–287

FEMALE-SPECIFIC NEUROPROTECTION AGAINST TRANSIENT BRAIN ISCHEMIA OBSERVED IN MICE DEVOID OF PRION PROTEIN IS ABOLISHED BY ECTOPIC EXPRESSION OF PRION PROTEIN-LIKE PROTEIN

Y. SAKURAI-YAMASHITA,[a1]* S. SAKAGUCHI,[b,c1] D. YOSHIKAWA,[b] N. OKIMURA,[b] Y. MASUDA,[a] S. KATAMINE[b] AND M. NIWA[a]

[a]*Department of Pharmacology 1, Nagasaki University Graduate School of Biomedical Sciences, 1-12-4 Sakamoto, Nagasaki 852-8523, Japan*

[b]*Department of Molecular Microbiology and Immunology, Nagasaki University Graduate School of Biomedical Sciences, 1-12-4 Sakamoto, Nagasaki 852-8523, Japan*

[c]*PRESTO, Japan Science and Technology Agency, 4-1-8 Honcho Kawaguchi, Saitama 332-0012, Japan*

Abstract—This study was designed to examine the function of cellular prion protein and prion protein-like protein/Doppel, in transient ischemia-related neuronal death in the hippocampus. Two different lines of mice devoid of cellular prion protein, Zrch I *Prnp*$^{0/0}$ and Ngsk *Prnp*$^{0/0}$, were used. The former lacks cellular prion protein whereas the latter ectopically expresses prion protein-like protein/Doppel in the brain in the absence of cellular prion protein. Mice were subjected to 10 min-occlusion of the bilateral common carotid arteries with recovery for 14 days. Less than 10% of the pyramidal neurons in the CA1 subfield were degenerated in male and female wild-type mice. In contrast, more than half of the neurons were lost in male Zrch I *Prnp*$^{0/0}$ and Ngsk *Prnp*$^{0/0}$ mice. Such severe neuronal loss was also observed in female Ngsk *Prnp*$^{0/0}$ mice. However, female Zrch I *Prnp*$^{0/0}$ mice showed mild neuronal loss similar to wild-type mice. Flunarizine, a T- and L-type Ca^{2+}-channel antagonist, significantly reduced the neuronal loss in female but not in male Ngsk *Prnp*$^{0/0}$ mice. These results indicate that loss of cellular prion protein renders hippocampal neurons susceptible to ischemic insult specifically in male but not female mice and the ectopic expression of prion protein-like protein/Doppel aggravates the ischemic neuronal death in female prion protein-null mice probably via overloading of Ca^{2+}-dependent signaling.

Key words: prion protein, prion protein-like protein, ischemia, hippocampus, neuronal death, mouse.

The cellular prion protein, PrP^C, is a gylcosylphosphatidylinositol (GPI)-anchored membrane glycoprotein abundantly expressed in the CNS, particularly by neurons (Prusiner, 1998; Weissmann et al., 2002). The conformational conversion of PrP^C into the pathogenic isoform, PrP^{Sc} (scrapie), via unknown post-translational modifications is thought to be an essential process in the pathogenesis of prion diseases, including Creutzfeldt-Jakob disease in humans, scrapie in sheep, and bovine spongiform encephalopathy in cattle (Prusiner, 1998; Weissmann et al., 2002). However, its normal function remains to be elucidated.

To explore the physiological functions of PrP^C, several lines of mice devoid of PrP^C (*Prnp*$^{0/0}$) have been independently established using different targeting strategies. Some lines of the mice, including Zrch I *Prnp*$^{0/0}$ and Npu *Prnp*$^{0/0}$, were reported to develop and grow without any neurological abnormalities (Bueler et al., 1992; Manson et al., 1994). In contrast, others, such as Ngsk *Prnp*$^{0/0}$ and Rcm0 *Prnp*$^{0/0}$, developed ataxia and Purkinje cell degeneration in old age due to the ectopic expression of a GPI-anchored prion protein-like protein, designated PrPLP/Doppel (Dpl), in their brains (Sakaguchi et al., 1996; Moore et al., 1999). Moore et al. (1999) also showed that PrPLP/Dpl is toxic not only to Purkinje cells but also to other types of neurons by demonstrating that Zrch I *Prnp*$^{0/0}$ mice highly expressing transgenic PrPLP/Dpl in their brains exhibited degenerative changes in Purkinje cells, cerebellar granule cells, and hippocampal pyramidal neurons (Moore et al., 2001). Interestingly, some of us demonstrated that the Purkinje cell degeneration in Ngsk *Prnp*$^{0/0}$ mice could be successfully rescued by re-introducing multiple copies of a transgene encoding PrP^C, indicating that PrP^C has the potential to abrogate the PrPLP/Dpl-induced neurotoxicity (Nishida et al., 1999). It was also recently reported that weight-drop contusional injury over the brain caused much severe neuronal damage in prion protein (PrP)-null mice (Hoshino et al., 2003). These results suggest that PrP^C is involved in the neuroprotection against certain neurodegenerative insults.

In the present study, we examined the roles of PrP^C and PrPLP/Dpl in the neuronal cell death induced by transient forebrain ischemia in two different lines of PrP-null mice, Zrch I *Prnp*$^{0/0}$ and Ngsk *Prnp*$^{0/0}$. We show that the lack of PrP^C increased susceptibility to the ischemic damage of the hippocampal CA1 neurons in male but not female mice and that the ectopic expression of PrPLP/Dpl disrupted the female-specific neuroprotective effect and induced ischemic neuronal death in female PrP-mutant mice. We also show that the ischemia-induced neuronal

[1] The first two authors equally contributed to this study.

*Corresponding author. Tel: +81-95-849-7043; fax: +81-95-849-7044.
E-mail address: yasukosy@net.nagasaki-u.ac.jp (Y. Sakurai-Yamashita).

Abbreviations: Dpl, Doppel; GPI, gylcosylphosphatidylinositol; MCA, middle cerebral artery; PrP, prion protein; PrP^C, cellular isoform of prion protein; PrPLP, prion protein-like protein; TUNEL, terminal deoxynucleotidyl transferase-mediated deoxyuridine nick end labeling.

0306-4522/05$30.00+0.00
doi:10.1016/j.neuroscience.2005.06.095

cell death in female but not male Ngsk $Prnp^{0/0}$ mice could be significantly mitigated by treatment with the Ca^{2+} channel antagonist flunarizine.

EXPERIMENTAL PROCEDURES

Animals

C57BL/6 mice were purchased from Japan SLC (Shizuoka, Japan). Ngsk $Prnp^{0/0}$ and Zrch I $Prnp^{0/0}$ mice were generated as previously described (Bueler et al., 1992; Sakaguchi et al., 1996). In the present study, Ngsk $Prnp^{0/0}$ mice carrying a mixed genetic background of 129Sv and C57BL/6 were backcrossed with C57BL/6 mice 12 times. Zrch I $Prnp^{0/0}$ mice were obtained by mating pairs of Zrch I $Prnp^{0/+}$ mice, which had been generated by crossing Zrch I $Prnp^{0/0}$ mice (129Sv×C57BL/6) with FVB wild-type mice. These mice were handled in accordance with the Guidelines of Animal Experimentation of Nagasaki University and also with the National Institutes of Health Guide for the Care and Use of Laboratory Animals (NIH Publications No. 80-23). All efforts were made to minimize the number of animals used and their suffering.

Surgical procedures

All experiments were carried out using 8–12 week old mice. Mice were anesthetized with 1.5% halothane in room air and kept at 37 °C on a heating pad during surgery. The bilateral common carotid arteries were surgically exposed and occluded for 10 min with aneurismal clips. The animals were allowed to recover for 14 days after recirculation.

Histology

The animals were deeply anesthetized and perfused intracardially with PBS followed by 4% paraformaldehyde. Coronal paraffin sections (6 μm thick) were stained with hematoxylin–eosin. Apoptotic cell death was evaluated using the terminal deoxynucleotidyl transferase-mediated deoxyuridine nick end labeling (TUNEL) staining method (*In situ* Cell Death Detection kit, Roche Diagnostics, Manheim, Germany).

Ischemic neuronal damage score

The ischemic neuronal damage in the pyramidal layer of the CA1 subfield was scored in a double blind manner as described previously with a few minor modifications (Sakurai-Yamashita et al., 2003). In brief, score 1 was defined as no neuronal loss, score 2 was <10% loss of the neurons, score 3 was 10–50% loss of the neurons, and score 4 was >50% loss of the neurons.

Drug treatment

Flunarizine (Sigma-Aldrich Co., St Louis, MO, USA) was intraperitoneally injected into female and male Ngsk $Prnp^{0/0}$ mice (0.5 mg/kg) 15 min before the onset of the occlusion, as well as 8 h and 24 h after reperfusion. Saline was injected as control. A pellet containing 0.025 mg 17β-estradiol (Innovative Research of America, Sarasota, FL, USA) was s.c. implanted into male Zrch I $Prnp^{0/0}$ mice under light anesthesia. This pellet is designed to constantly release 17β-estradiol for 21 days. Seven days after implantation of the pellet, the mice underwent surgery with recovery for 14 days. Serum was taken from the mice just before kill and the concentration of 17β-estradiol measured. Control group mice were treated identically to the 17β-estradiol group mice except for the implantation of the pellet containing 17β-estradiol.

Table 1. Ischemia-related neuronal damage in PrP-null mice

Mouse	Score			
	1	2	3	4
Male				
Wild-type (4)	3	1	0	0
Zrch I $Prnp^{0/0}$ (5)*	0	0	2	3
Ngsk $Prnp^{0/0}$ (3)*	0	0	2	1
Female				
Wild-type (4)	1	3	0	0
Zrch I $Prnp^{0/0}$ (5)	2	2	0	1
Ngsk $Prnp^{0/0}$ (5)*	1	0	0	4

* Represents significant difference ($P<0.05$) from wild-type animals using analysis of variance (Kruskal-Wallis test) followed by the Mann-Whitney *U*-test. The numbers in parentheses show the number of animals analyzed.

Statistics

All data are presented as the ischemic neuronal damage score. The score was analyzed by the Kruskal-Wallis test followed by the Mann-Whitney *U* test.

RESULTS

Transient brain ischemia causes mild neuronal damage in wild-type mice

We subjected four male and four female wild-type C57BL/6 mice to 10 min-transient occlusion of the common carotid arteries. The ischemia-induced neuronal damage was scored from 1 to 4 on the basis of the degree of the neuronal loss in the hippocampal CA1 subfield (Table 1). Three male mice and one female mouse showed no neuronal loss in the CA1 subfield (score 1, Fig. 1A) and the others developed only <10% loss of the CA1 neurons (score 2, Fig. 1B). Male wild-type mice seemed to be slightly resistant to the ischemia compared with female mice, but no significant difference in the scores could be detected between male and female wild-type mice. Moreover, no difference in the expression levels of PrP^C in the hippocampus could be observed between non-ischemic male and female wild-type mice on Western blotting (data not shown). These results indicate that the CA1 neurons of wild-type mice tolerate 10 min-transient global brain ischemia well.

Ischemic neuronal damage is increased in male but not female PrP-null mice

To examine the neuroprotective function of PrP^C in the brain ischemia, Zrch I $Prnp^{0/0}$ mice were similarly subjected to 10 min-brain ischemia. In contrast to wild-type mice, all male Zrch I $Prnp^{0/0}$ mice exhibited marked neuronal loss in the CA1 region, showing a high ischemic neuronal damage score of 3 or 4 (Table 1). Three mice showed a neuronal loss of more than half (Fig. 1C) and the other two mice showed 10–50% neuronal loss. These scores of the male PrP-mutant mice were significantly increased compared with those of wild-type mice ($P<0.05$, Table 1). However, the neuronal damage score was not increased in female Zrch I $Prnp^{0/0}$ mice (Table 1). Most of the female mice

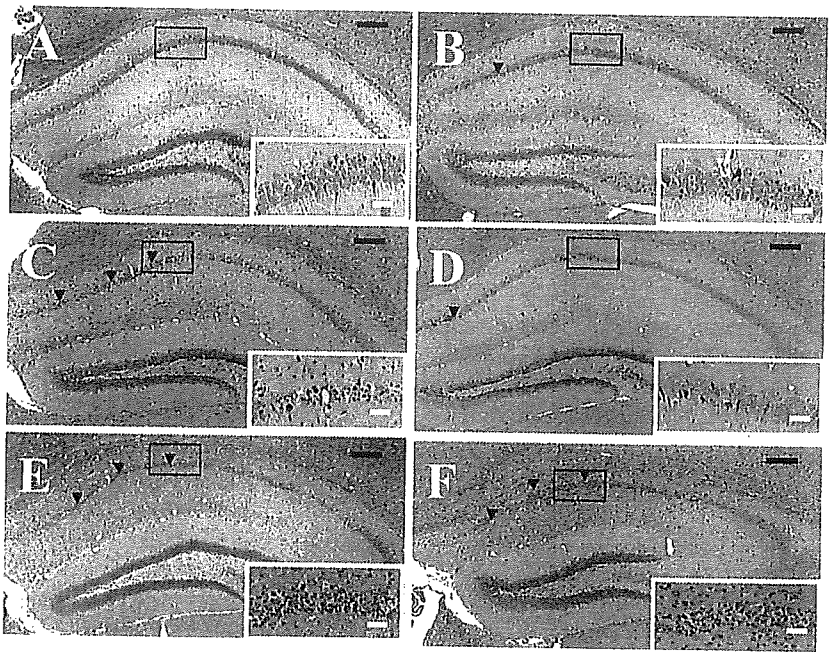

Fig. 1. Representative photographs of the hippocampus of each mouse strain exposed to a transient global ischemia. All mice were subjected to carotid artery occlusion for 10 min with recovery for 14 days. Paraffinized coronal sections (6 μm in thickness) were stained with hematoxylin–eosin. (A) No neuronal loss, score 1, was observed in the wild-type male mice. (B) A small neuronal loss in the CA1 subfield, score 2, was detected in the wild-type female mice. (C) More than half of the neurons in the CA1 subfield were lost in the Zrch I *Prnp*$^{o/o}$ male mice, with score 4. (D) A small neuronal loss in the CA1 subfield, score 2, was also observed in the Zrch I *Prnp*$^{o/o}$ female mice. (E) More than half of the neurons in the CA1 subfield were lost in the Ngsk *Prnp*$^{o/o}$ male mice, with score 4. (F) Neuronal loss in more than half of the CA1 subfield, score 4, was observed in the most of the Ngsk *Prnp*$^{o/o}$ female mice. Arrowheads in photographs indicate the degenerated areas of the CA1 subfield. The photograph in the inset is the magnified region surrounded by a square in the CA1 subfield. Scale bar=500 μm (A–F); and 200 μm in the insets.

developed no or mild neuronal loss in the CA1 region after 10 min-forebrain ischemia (Fig. 1D). Only one mouse suffered from severe neuronal damage with a score of 4 (Table 1).

Ischemic neuronal damage is increased in female PrP-null mice ectopically expressing PrPLP/Dpl

To examine the influence of the ectopic expression of PrPLP/Dpl on brain ischemia in the absence of PrP^{C}, we subjected PrPLP/Dpl-expressing Ngsk *Prnp*$^{o/o}$ mice to 10 min-forebrain ischemia. Increased susceptibility of CA1 neurons to the ischemia could be detected in both male and female mutant mice (Table 1, Fig. 1E and F). All three male Ngsk *Prnp*$^{o/o}$ mice showed high ischemic neuronal damage scores of 3 or 4. These scores were similar to those of male Zrch I *Prnp*$^{o/o}$ mice and significantly higher than those of wild-type mice ($P<0.05$). Interestingly, female Ngsk *Prnp*$^{o/o}$ mice also developed similar marked neuronal loss in the CA1 subfield. Four out of five female Ngsk *Prnp*$^{o/o}$ mice showed the severe neuronal damage score of 4 but the one remaining female mouse exhibited no neuronal loss in the CA1 region (score 1).

Increased TUNEL-positive neurons are correlated with the ischemic neuronal loss in PrP-null mice

To understand the mechanism of the ischemic neuronal loss in PrP-null mice, hippocampal slices from the mice which received the 10 min-transient forebrain ischemia were subjected to TUNEL staining. No TUNEL-positive neurons could be detected in the CA1 subfield of control C57BL/6 mice showing score 1 (Fig. 2A). In contrast, a

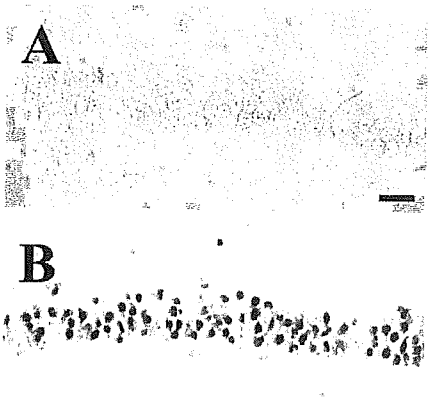

Fig. 2. Photographs of TUNEL-staining in the CA1 pyramidal layer of mice exposed to a transient global ischemia. Mice were subjected to carotid artery occlusion for 10 min with recovery for 14 days. Paraffinized coronal sections (6 μm in thickness) were stained by the TUNEL method. (A) No positive cells were observed in the wild-type male mice showing score 1. (B) Most of the cells of the CA1 pyramidal layer were TUNEL-positive in the Zrch I *Prnp*$^{o/o}$ male mice showing score 4. The number of the TUNEL-staining cells in the CA1 subfield was correlated with the neuronal damage score. Scale bar=100 μm (A).

Table 2. Ischemia-related neuronal damage in Zrch I $Prnp^{0/0}$ male mice

Treatment	Score			
	1	2	3	4
Sham-operated group (2)	0	0	0	2
Estradiol-implanted group (4)	0	0	1	3

The numbers in parentheses show the number of animals analyzed.

large number of the CA1 neurons were positively stained by TUNEL in male Zrch I $Prnp^{0/0}$ mice (Fig. 2B). Moreover, the CA1 neurons of both male and female Ngsk $Prnp^{0/0}$ mice were similarly stained by TUNEL (data not shown). We also examined the expression levels of anti-apoptotic protein Bcl-2 in the hippocampus of these two lines of non-ischemic $Prnp^{0/0}$ mice by Western blotting. Considerable amounts of the protein were similarly expressed in these $Prnp^{0/0}$ mice irrespective of their genders (data not shown).

Estradiol fails to rescue male PrP-null mice from ischemic neuronal damage

To investigate the possibility that neuroprotection against transient ischemia in female Zrch I $Prnp^{0/0}$ mice could be attributable to reproductive hormones, we first measured the levels of serum estradiol in three female mice from each group of wild-type, Zrch I $Prnp^{0/0}$, and Ngsk $Prnp^{0/0}$ mice. No significant difference in the levels (ranging from less than 10–16 pg/ml (data not shown)) could be detected between these groups. We next s.c. implanted a pellet of estradiol into each of four male Zrch I $Prnp^{0/0}$ mice and 7 days later subjected these mice to the transient brain ischemia. They showed higher concentration of serum estradiol than female Zrch I $Prnp^{0/0}$ mice (data not shown).

Two sham-operated male Zrch I $Prnp^{0/0}$ mice showed severe neuronal damages of score 4 (Table 2), similarly to non-treated mice. Indistinguishable damage was also observed in the estradiol-treated mice. Three out of four mice developed score 4 damage whereas the remaining one showed score 3 damage (Table 2).

Ca^{2+}-channel antagonist flunarizine mitigates ischemic neuronal damage in female but not male PrP-null mice expressing PrPLP/Dpl

The effect of the T- and L-type Ca^{2+}-channel antagonist flunarizine on the ischemic neuronal damage was examined in PrP-mutant mice. Flunarizine (0.5 mg/kg of mouse weight) was intraperitoneally injected into six female and four male Ngsk $Prnp^{0/0}$ mice 15 min before the onset of 10 min-occlusion of the common carotid arteries as well as 8 h and 24 h after the reperfusion. Saline was injected as control. Five out of seven control female mice developed severe neuronal damage (score 4) while the other 2 showed mild neurodegeneration (score 2). However, the ischemic neuronal damage score of the flunarizine-administered group was significantly lower than that of the control group ($P<0.05$, Fig. 3A). In four of six flunarizine-administered female mice, the neuronal damage score was 1 and TUNEL-positive neurons could not be detected in the CA1 region (data not shown). Only the two remaining mice showed scores of 3 and 4, respectively. On the other hand, the treatment could not rescue hippocampal neurons from the ischemic damages in male Ngsk $Prnp^{0/0}$ mice (Fig. 3B). The three flunarizine-administered mice exhibited severe damage scores of 3 and 4 and only one mouse showed no neuronal damage. Control group of mice also showed damage scores of 3 and 4.

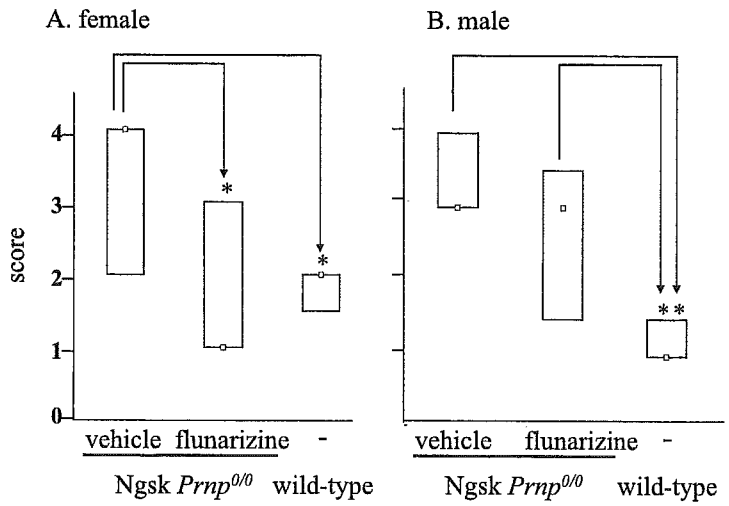

Fig. 3. Effect of flunarizine on the neuronal loss induced by transient global ischemia in the Ngsk $Prnp^{0/0}$ male and female mice. Flunarizine (0.5 mg/kg) was injected 15 min before the occlusion, as well as 8 and 24 h after reperfusion. (A) Flunarizine significantly reduced the neuronal damage score in the Ngsk $Prnp^{0/0}$ female mice [$P<0.05$ by analysis of variance (Kruskal-Wallis test) followed by Mann-Whitney U test]. The scores of the flunarizine-treated Ngsk $Prnp^{0/0}$ female mice and wild-type female mice were not significantly different. The small square in the box is the median, and 25–75% of the score is in the box. (B) Flunarizine did not reduce the neuronal damage score in the Ngsk $Prnp^{0/0}$ male mice.

DISCUSSION

The present study demonstrated that the susceptibility of hippocampal CA1 neurons to transient forebrain ischemia was markedly increased in male Zrch I *Prnp*$^{0/0}$ mice compared with that in control C57BL/6 wild-type mice. McLennan et al. (2004) also recently reported that permanent occlusion of the middle cerebral artery (MCA) increased the infarction volume in male PrP-null mice compared with wild-type mice. These results indicate that PrP^{C} is involved in neuroprotection against brain ischemia. However, no increased susceptibility could be detected in female Zrch I *Prnp*$^{0/0}$ mice, suggesting an interesting possibility that the neuroprotective function of PrP^{C} could be masked by female-specific neuroprotective factor(s). We also demonstrated that, in contrast to the case of Zrch I *Prnp*$^{0/0}$ mice, both male and female Ngsk *Prnp*$^{0/0}$ mice exhibited severe ischemic damage to CA1 neurons. Since Ngsk *Prnp*$^{0/0}$ mice ectopically express PrPLP/Dpl in their brains, especially in neurons (Li et al., 2000), this result strongly suggests that PrPLP/Dpl could counteract the female-specific neuroprotective function observed in Zrch I *Prnp*$^{0/0}$ mice, increasing the susceptibility of PrP^{C}-deficient neurons to ischemic insults.

It was shown that the expression of PrP^{C} was upregulated in the damaged brains of wild-type mice exposed to permanent focal ischemia and in the penumbra neurons damaged by infarction of human brain (McLennan et al., 2004). However, we failed to detect the upregulated expression of PrP^{C} in the hippocampus of wild-type mice 24 h after the transient ischemia (data not shown). Weise et al. (2004) also reported that transient (60 min) but not permanent occlusion of the MCA could not increase PrP^{C} in the ischemic brain hemisphere of wild-type mice. Permanent brain ischemia results in more severe neuronal damage than transient ischemia, leading to larger infarcts in the affected brain (Weise et al., 2004). It is therefore conceivable that, to survive long-term ischemia, neurons might require stronger neuroprotective signals and therefore stimulate the expression of PrP^{C}.

Pyramidal neurons in the hippocampus are vulnerable to transient forebrain ischemia and degenerate in the process of delayed neuronal death (Kirino 1982). Some of us and others previously showed that CA1 neurons are highly sensitive to transient global ischemia in rodents, including gerbils and rats (Kirino, 1982; Pulsinelli et al., 1982; Yamashita et al., 1993, 1994). In the present study, we also failed to detect any neuronal cell loss in the other hippocampal subfields, such as CA2, CA3 and dentate gyrus of C57BL/6 and PrP-null mice when no ischemic cell damage to CA1 neurons was observed. Wellons et al. (2000) have previously suggested that scoring of neuronal loss in the CA1 subfield is rational for the estimation of global ischemia-related neuronal damage. Thus, we evaluated the transient ischemia-related brain damage by the loss of neurons in the CA1 subfield of these mice.

Different susceptibility to brain ischemia has been demonstrated among different mouse strains (Fujii et al., 1997; Yang et al., 1997; Wellons et al., 2000). C57BL/6 mice are the most susceptible to transient global ischemia because of incomplete formation of the circle of Willis (Yang et al., 1997; Wellons et al., 2000). Ngsk *Prnp*$^{0/0}$ mice were back-crossed with C57BL/6 mice for 12 generations. On the other hand, Zrch I *Prnp*$^{0/0}$ mice still carry a mixed background of C57BL/6, 129Sv, and FVB lines. Both PrP-null lines of male mice showed similar susceptibility of their CA1 neurons to transient ischemia, suggesting that the influence of genetic background could be subtle on the consequences of this type of transient ischemia in these mice. However, we cannot completely exclude genetic influences on the different susceptibility to transient ischemia between Zrch I *Prnp*$^{0/0}$ and Ngsk *Prnp*$^{0/0}$ mice.

Treatment with female sex hormones, estrogens or progesterones, has been demonstrated to reduce ischemia-induced injury and enhance functional recovery after MCA occlusion in rodents (Dubal et al., 1998; Toung et al., 1998; Murphy et al., 2002, 2004; Gibson and Murphy, 2004), suggesting that these sex hormones are involved in the female-specific neuroprotection observed in Zrch I *Prnp*$^{0/0}$ mice. However, estradiol, a major estrogen, could be detected at similar levels in the sera of female wild-type, Zrch I *Prnp*$^{0/0}$ mice and Ngsk *Prnp*$^{0/0}$ mice, and failed to rescue male Zrch I *Prnp*$^{0/0}$ mice from the ischemic neuronal damage in the hippocampus. These results suggest that estrogens are unlikely to be involved in the female-specific protection of CA1 neurons in Zrch I *Prnp*$^{0/0}$ mice. Knockout of estrogen signals in female Zrch I *Prnp*$^{0/0}$ mice by mating with mice deficient for the estrogen signals could be very useful to elucidate the exact involvement of estrogens in the neuroprotection in mice.

The TUNEL-positive CA1 neurons were increased proportionally to the ischemic neuronal loss in PrP-null mice, suggesting that the exacerbated ischemic loss of the neurons in these mice could be due to increased vulnerability of the neurons to apoptosis. Dysregulated excess of intracellular Ca^{2+} has been shown to be critically involved in the ischemia-induced apoptosis of neurons (Pisani et al., 2004). Abnormal Ca^{2+}-activated K^{+} currents were reported in hippocampal pyramidal neurons of Zrch I *Prnp*$^{0/0}$ mice and the mutant mice showed altered intracellular Ca^{2+} in cerebellar granule cells (Colling et al., 1996; Herms et al., 2000), indicating that PrP^{C} could be involved in the regulation of Ca^{2+} homeostasis in neurons. It is therefore conceivable that increased susceptibility of the PrP^{C}-deficient neurons to transient ischemia could be attributable to the dysregulation of intracellular Ca^{2+}. We demonstrated that the T- and L-type Ca^{2+}-antagonist, flunarizine, significantly reduced the ischemic neuronal damage score in female but not male Ngsk *Prnp*$^{0/0}$ mice, suggesting that the Ca^{2+}-dependent signaling load in neurons is different between male and female mice. Indeed, it was previously reported that Ca^{2+}/calmodulin-dependent protein kinase activity in mouse cardiac myocytes was different in different genders, being significantly greater in males compared with females (Konhilas et al., 2001). Taken together, it could be conceivable that loss of PrP^{C} renders neurons susceptible to transient ischemia in a male-specific manner probably via dysregulating ho-

meostasis of intracellular Ca^{2+} more in males than in females, and that the ectopic expression of PrPLP/Dpl increases the intracellular Ca^{2+} load in female PrP-null mice, enhancing the susceptibility of their neurons to transient ischemia.

Oxidative stress is also known to be involved in ischemic neuronal damage. Several reports showed that PrP^C could be involved in the inactivation of oxidative stress by regulating Cu^{2+}-dependent anti-oxidant enzymes, including Cu/Zn superoxide dismutase (Brown et al., 1997, 2002). In contrast, PrPLP/Dpl is suggested to associate with the pro-oxidative cascade (Wong et al., 2001; Cui et al., 2003). It is therefore alternatively conceivable that the neuroprotective function of PrP^C against transient brain ischemia could be mediated by inactivation of oxidative stress, and that the increased susceptibility to the ischemia in PrPLP/Dpl-expressing PrP-null mice could be attributable to excessive oxidative stress. Moreover, Kuwahara et al. (1999) previously reported that apoptosis induced by serum withdrawal in cultured PrP-deficient hippocampal neurons could be prevented by the expression of either PrP^C or the anti-apoptotic molecule, Bcl-2. Therefore, it is also possible that the neuroprotective function of PrP^C might involve the anti-apoptotic pathway and PrPLP/Dpl could be a pro-apoptotic molecule. We could not detect any difference in the expression levels of Bcl-2 in the hippocampus between female Zrch I $Prnp^{o/o}$ and Ngsk $Prnp^{o/o}$ mice, suggesting that Bcl-2 is unlikely to be involved in the neuroprotection in female Zrch I $Prnp^{o/o}$ mice.

It has been postulated that the functional loss of PrP^C is partly involved in the pathogenesis of prion diseases (Collinge et al., 1994; Sakaguchi et al., 1996; Tobler et al., 1996), but the exact molecular pathogenesis remains unknown. Thus, elucidation of the neuroprotective function of PrP^C against brain ischemia could be helpful for further understanding the molecular pathogenesis of prion diseases.

Acknowledgments—We all thank Prof. Stanley B. Prusiner and Dr. Patrick Tremblay for providing Zrch I $Prnp^{o/o}$ mice. This study was supported in part by a Research on Specific Diseases grant from the Ministry of Health, Labor and Welfare, Japan.

REFERENCES

Brown DR, Nicholas RS, Canevari L (2002) Lack of prion protein expression results in a neuronal phenotype sensitive to stress. J Neurosci Res 67:211–224.

Brown DR, Schulz-Schaeffer WJ, Schmidt B, Kretzschmar HA (1997) Prion protein-deficient cells show altered response to oxidative stress due to decreased SOD-1 activity. Exp Neurol 146:104–112.

Bueler H, Fischer M, Lang Y, Bluethmann H, Lipp HP, DeArmond SJ, Prusiner SB, Aguet M, Weissmann C (1992) Normal development and behaviour of mice lacking the neuronal cell-surface PrP protein. Nature 356:577–582.

Colling SB, Collinge J, Jefferys JG (1996) Hippocampal slices from prion protein null mice: disrupted Ca(2+)-activated K+ currents. Neurosci Lett 209:49–52.

Collinge J, Whittington MA, Sidle KC, Smith CJ, Palmer MS, Clarke AR, Jefferys JG (1994) Prion protein is necessary for normal synaptic function. Nature 370:295–297.

Cui T, Holme A, Sassoon J, Brown DR (2003) Analysis of doppel protein toxicity. Mol Cell Neurosci 23:144–155.

Dubal DB, Kashon ML, Pettigrew LC, Ren JM, Finklestein SP, Rau SW, Wise PM (1998) Estradiol protects against ischemic injury. J Cereb Blood Flow Metab 18:1253–1258.

Fujii M, Hara H, Meng W, Vonsattel JP, Huang Z, Moskowitz MA (1997) Strain-related differences in susceptibility to transient forebrain ischemia in SV-129 and C57black/6 mice. Stroke 28:1805–1810; discussion 1811.

Gibson CL, Murphy SP (2004) Progesterone enhances functional recovery after middle cerebral artery occlusion in male mice. J Cereb Blood Flow Metab 24:805–813.

Herms JW, Korte S, Gall S, Schneider I, Dunker S, Kretzschmar HA (2000) Altered intracellular calcium homeostasis in cerebellar granule cells of prion protein-deficient mice. J Neurochem 75: 1487–1492.

Hoshino S, Inoue K, Yokoyama T, Kobayashi S, Asakura T, Teramoto A, Itohara S (2003) Prions prevent brain damage after experimental brain injury: a preliminary report. Acta Neurochir Suppl 86:297–299.

Kirino T (1982) Delayed neuronal death in the gerbil hippocampus following ischemia. Brain Res 239:57–69.

Konhilas JP, Maass AH, Luckey SW, Stauffer BL, Olson EN, Leinwand LA (2001) Sex modifies exercise and cardiac adaptation in mice. Am J Physiol Heart Circ Physiol 287:2768–2776.

Kuwahara C, Takeuchi AM, Nishimura T, Haraguchi K, Kubosaki A, Matsumoto Y, Saeki K, Yokoyama T, Itohara S, Onodera T (1999) Prions prevent neuronal cell-line death. Nature 400:225–226.

Li A, Sakaguchi S, Atarashi R, Roy BC, Nakaoke R, Arima K, Okimura N, Kopacek J, Shigematsu K (2000) Identification of a novel gene encoding a PrP-like protein expressed as chimeric transcripts fused to PrP exon 1/2 in ataxic mouse line with a disrupted PrP gene. Cell Mol Neurobiol 20:553–567.

Manson JC, Clarke AR, Hooper ML, Aitchison L, McConnell I, Hope J (1994) 129/Ola mice carrying a null mutation in PrP that abolishes mRNA production are developmentally normal. Mol Neurobiol 8:121–127.

McLennan NF, Brennan PM, McNeill A, Davies I, Fotheringham A, Rennison KA, Ritchie D, Brannan F, Head MW, Ironside JW, Williams A, Bell JE (2004) Prion protein accumulation and neuroprotection in hypoxic brain damage. Am J Pathol 165:227–235.

Moore RC, Lee IY, Silverman GL, Harrison PM, Strome R, Heinrich C, Karunaratne A, Pasternak SH, Chishti MA, Liang Y, Mastrangelo P, Wang K, Smit AF, Katamine S, Carlson GA, Cohen FE, Prusiner SB, Melton DW, Tremblay P, Hood LE, Westaway D (1999) Ataxia in prion protein (PrP)-deficient mice is associated with upregulation of the novel PrP-like protein doppel. J Mol Biol 292:797–817.

Moore RC, Mastrangelo P, Bouzamondo E, Heinrich C, Legname G, Prusiner SB, Hood L, Westaway D, DeArmond SJ, Tremblay P (2001) Doppel-induced cerebellar degeneration in transgenic mice. Proc Natl Acad Sci U S A 98:15288–15293.

Murphy SJ, Littleton-Kearney MT, Hurn PD (2002) Progesterone administration during reperfusion, but not preischemia alone, reduces injury in ovariectomized rats. J Cereb Blood Flow Metab 22: 1181–1188.

Murphy SJ, McCullough LD, Smith JM (2004) Stroke in the female: role of biological sex and estrogen. ILAR J 45:147–159.

Nishida N, Tremblay P, Sugimoto T, Shigematsu K, Shirabe S, Petromilli C, Erpel SP, Nakaoke R, Atarashi R, Houtani T, Torchia M, Sakaguchi S, DeArmond SJ, Prusiner SB, Katamine S (1999) A mouse prion protein transgene rescues mice deficient for the prion protein gene from Purkinje cell degeneration and demyelination. Lab Invest 79:689–697.

Pisani A, Bonsi P, Calabresi P (2004) Calcium signaling and neuronal vulnerability to ischemia in the striatum. Cell Calcium 36:277–284.

Prusiner SB (1998) Prions. Proc Natl Acad Sci U S A 95:13363–13383.

Pulsinelli WA, Waldman S, Rawlinson D, Plum F (1982) Moderate hyperglycemia augments ischemic brain damage: a neuropathologic study in the rat. Neurology 32:1239–1246.

Sakaguchi S, Katamine S, Nishida N, Moriuchi R, Shigematsu K, Sugimoto T, Nakatani A, Kataoka Y, Houtani T, Shirabe S, Okada H, Hasegawa S, Miyamoto T, Noda T (1996) Loss of cerebellar Purkinje cells in aged mice homozygous for a disrupted PrP gene. Nature 380:528–531.

Sakurai-Yamashita Y, Yamashita K, Niwa M, Taniyama K (2003) Involvement of 5-hydroxytryptamine4 receptor in the exacerbation of neuronal loss by psychological stress in the hippocampus of SHRSP with a transient ischemia. Brain Res 973:92–98.

Tobler I, Gaus SE, Deboer T, Achermann P, Fischer M, Rulicke T, Moser M, Oesch B, McBride PA, Manson JC (1996) Altered circadian activity rhythms and sleep in mice devoid of prion protein. Nature 380:639–642.

Toung TJ, Traystman RJ, Hurn PD (1998) Estrogen-mediated neuroprotection after experimental stroke in male rats. Stroke 29: 1666–1670.

Weise J, Crome O, Sandau R, Schulz-Schaeffer W, Bahr M, Zerr I (2004) Upregulation of cellular prion protein (PrPc) after focal cerebral ischemia and influence of lesion severity. Neurosci Lett 372:146–150.

Weissmann C, Enari M, Klohn PC, Rossi D, Flechsig E (2002) Molecular biology of prions. Acta Neurobiol Exp (Wars) 62:153–166.

Wellons JC 3rd, Sheng H, Laskowitz DT, Burkhard Mackensen G, Pearlstein RD, Warner DS (2000) A comparison of strain-related susceptibility in two murine recovery models of global cerebral ischemia. Brain Res 868:14–21.

Wong BS, Liu T, Paisley D, Li R, Pan T, Chen SG, Perry G, Petersen RB, Smith MA, Melton DW, Gambetti P, Brown DR, Sy MS (2001) Induction of HO-1 and NOS in doppel-expressing mice devoid of PrP: implications for doppel function. Mol Cell Neurosci 17: 768–775.

Yamashita K, Kataoka Y, Niwa M, Shigematsu K, Himeno A, Koizumi S, Taniyama K (1993) Increased production of endothelins in the hippocampus of stroke-prone spontaneously hypertensive rats following transient forebrain ischemia: histochemical evidence. Cell Mol Neurobiol 13:15–23.

Yamashita K, Niwa M, Kataoka Y, Shigematsu K, Himeno A, Tsutsumi K, Nakano-Nakashima M, Sakurai-Yamashita Y, Shibata S, Taniyama K (1994) Microglia with an endothelin ETB receptor aggregate in rat hippocampus CA1 subfields following transient forebrain ischemia. J Neurochem 63:1042–1051.

Yang G, Kitagawa K, Matsushita K, Mabuchi T, Yagita Y, Yanagihara T, Matsumoto M (1997) C57BL/6 strain is most susceptible to cerebral ischemia following bilateral common carotid occlusion among seven mouse strains: selective neuronal death in the murine transient forebrain ischemia. Brain Res 752:209–218.

(Accepted 30 June 2005)
(Available online 28 September 2005)